

Magnetic moments of the spin- $\frac{3}{2}$ singly heavy baryons

Lu Meng,^{1,*} Guang-Juan Wang,^{1,†} Chang-Zhi Leng,^{1,‡} Zhan-Wei Liu,^{2,§} and Shi-Lin Zhu^{1,3,¶}

¹*School of Physics and State Key Laboratory of Nuclear Physics and Technology, Peking University, Beijing 100871, China*

²*School of Physical Science and Technology, Lanzhou University, Lanzhou 730000, China*

³*Collaborative Innovation Center of Quantum Matter, Beijing 100871, China*

We calculate the magnetic moments of spin- $\frac{3}{2}$ singly charmed baryons in the heavy baryon chiral perturbation theory (HBChPT). The analytical expressions are given up to $\mathcal{O}(p^3)$. The heavy quark symmetry is used to reduce the number of low energy constants (LECs). With the lattice QCD simulation data as the magnetic moments of the charmed baryons, the numerical results are given up to $\mathcal{O}(p^3)$ in three scenarios. In the first scenario, we use the results in the quark model as the leading order input. In the second scenario, we use the heavy quark symmetry and neglect the contribution of heavy quark. In the third scenario, the heavy quark contribution is considered on the basis of the scenario II and the magnetic moments of singly bottom baryons are given as a by-product.

I. INTRODUCTION

The singly heavy baryon contains a heavy quark and two light quarks. The two light quarks form the $\bar{3}_f$ and the 6_f representation in the SU(3) flavor symmetry. With the constraint of Fermi-Dirac statistics, the spin of the $\bar{3}_f$ and the 6_f diquarks are 0 and 1, respectively. Thus, the total spin of the $\bar{3}_f$ heavy baryon is $\frac{1}{2}$ while that of the 6_f heavy baryon is either $\frac{1}{2}$ or $\frac{3}{2}$.

The electromagnetic form factors are important properties of the hadrons, which can reveal their inner structures. The magnetic moments of hadrons especially attract much attention from the theorists and experimentalists [1–7]. The magnetic moments of the singly charmed baryons were investigated in naive quark model in Ref. [8]. In Ref. [9], the relativistic effect was considered. The magnetic moments and charge radii of the charmed baryons are calculated [9]. The SU(4) chiral constituent quark model was also adopted to calculate the (transition) magnetic moments of spin- $\frac{1}{2}$ and spin- $\frac{3}{2}$ charmed baryons [10]. The masses and magnetic moments of heavy flavor baryons were calculated in hyper central model in Ref. [11]. The magnetic moments of spin- $\frac{3}{2}$ heavy baryons were obtained using the effective mass and screened charge scheme [12]. Besides the above quark models, the MIT bag model was employed to get the magnetic moments of heavy baryons [13], which were reexamined in Ref. [14]. The magnetic moments of charmed baryons were calculated in the skyrmion description [15]. The mass and magnetic moments of the heavy flavored baryons were calculated in the QCD sum rules [16–18]. The magnetic moments of the lowest-lying singly heavy baryons were investigated in the chiral quark-soliton model [19]. The (transition) magnetic moments and charge radii of charmed baryons were simulated with the lattice QCD recently [20–23].

The chiral perturbation theory (ChPT) is a model-independent method to study the hadron properties [24–26]. When one performs the ChPT in the baryon sector, the nonvanishing baryon mass in chiral limit will mess up the power counting used in the pure meson sector. The heavy baryon chiral perturbation theory (HBChPT) was introduced to solve the problem [27, 28]. The HBChPT is expanded by the momenta of pseudoscalar mesons and the residual momenta of heavy baryons. The HBChPT was widely performed to calculate the electromagnetic properties of baryons. The magnetic moments of octet and decuplet baryons were calculated in HBChPT scheme [29–34]. The (transition) magnetic moments of doubly heavy baryons were investigated in Refs. [35–37]. The magnetic moments of singly charmed baryons were calculated up to the next-to-next-to-leading order in HBChPT [38, 39]. In our recent work, we calculated the magnetic moments of spin- $\frac{1}{2}$ singly charmed baryons up to the $\mathcal{O}(p^3)$ [40].

The dynamics of singly heavy hadron is constrained by both the chiral symmetry in light quark sector and heavy quark symmetry in heavy quark sector. The heavy quark symmetry and the chiral symmetry were often combined to investigate the singly heavy hadrons. In Ref. [41], the authors constructed the chiral Lagrangians of heavy mesons

*Electronic address: lmeng@pku.edu.cn

†Electronic address: wgj@pku.edu.cn

‡Electronic address: lengchangzhi@pku.edu.cn

§Electronic address: liuzhanwei@lzu.edu.cn

¶Electronic address: zhushl@pku.edu.cn

($Q\bar{q}$) and heavy baryons (Qqq) and calculated their strong and semileptonic weak decays incorporating with heavy quark symmetry. The decay properties of singly heavy hadrons were calculated in a formalism which combines the chiral symmetry and the heavy quark symmetry [42–47]. The electromagnetic decays of $D_{s0}(2317)$ and $D_{s1}(2460)$ are investigated in the heavy-hadron chiral perturbation theory with the heavy quark symmetry [48].

In this work, we calculate the magnetic moments of the spin- $\frac{3}{2}$ singly heavy baryons in the HBChPT scheme. In Section II, we perform the multiple expansion of the electromagnetic current matrix element for spin- $\frac{3}{2}$ baryons. In Section III, we construct the Lagrangians used in calculating the magnetic moments. In Section IV, we calculate the analytical expressions of the magnetic moments order by order up to $\mathcal{O}(p^3)$. In Section V, we reduce the numbers of independent LECs in our analytical results with the heavy quark spin symmetry. We give the numerical results in three scenarios in Section VI. Some discussions and a brief conclusion are given in the Section VII. The integrals used in this work and some by-products are listed in the Appendix.

II. ELECTROMAGNETIC FORM FACTORS OF THE SPIN- $\frac{3}{2}$ BARYONS

Constrained by the time reversal (T), the parity (P), charge conjugate (C) and the gauge invariance, the matrix element of the electromagnetic current for spin- $\frac{3}{2}$ particles takes the following form [49, 50],

$$\langle T(p') | J_\mu | T(p) \rangle = \bar{u}^\rho(p') \mathcal{O}_{\rho\mu\sigma}(p', p) u^\sigma(p), \quad (1)$$

with

$$\mathcal{O}_{\rho\mu\sigma}(p', p) = -g_{\rho\sigma} \left[\gamma_\mu F_1(q^2) + \frac{i\sigma_{\mu\alpha} q^\alpha}{2M_T} F_2(q^2) \right] - \frac{q_\rho q_\sigma}{4M_T^2} \left[\gamma_\mu F_3(q^2) + \frac{i\sigma_{\mu\alpha} q^\alpha}{2M_T} F_4(q^2) \right], \quad (2)$$

where p and p' are the momenta of the spin- $\frac{3}{2}$ baryons. $P = p + p'$, $q = p' - p$. M_T is the baryon mass and u_σ is the Rarita-Schwinger spinor [51].

The charge (E0), electro-quadrupole (E2), magnetic-dipole (M1), and magnetic octupole (M3) form factors read

$$\begin{cases} G_{E0}(q^2) = F_1 - \tau F_2 + \frac{2}{3}\tau G_{E2}, \\ G_{E2}(q^2) = F_1 - \tau F_2 - \frac{1}{2}(1 + \tau)(F_3 - \tau F_4), \\ G_{M1}(q^2) = F_1 + F_2 + \frac{4}{5}\tau G_{M3}, \\ G_{M3}(q^2) = F_1 + F_2 - \frac{1}{2}(1 + \tau)(F_3 + F_4). \end{cases} \quad (3)$$

where $\tau = -\frac{q^2}{(2M_T)^2}$. On the right-hand side, we omit the variable q^2 of F_i for convenience. The magnetic-dipole form factor is related to the magnetic moment as

$$\mu_T = G_{M1}(0) \frac{e}{2M_T}. \quad (4)$$

In HBChPT scheme, The baryon momentum p^μ is decomposed into the $M_T v^\mu$ and a residual momentum k^μ , where v_μ is the velocity of the baryon and $v^2 = 1$. The baryon field T is decomposed into a “light” field $\mathcal{T}(x)$ and a “heavy” field $\mathcal{N}(x)$,

$$\mathcal{T}(x) = e^{iM_T v \cdot x} \frac{1+\not{v}}{2} T(x), \quad (5)$$

$$\mathcal{N}(x) = e^{iM_T v \cdot x} \frac{1-\not{v}}{2} T(x). \quad (6)$$

After integrating out the heavy degrees of freedom, one gets the nonrelativistic Lagrangians. In the HBChPT scheme, the theory is expanded by either the momenta of the pseudoscalar mesons or the residual momenta of the baryons.

In the HBChPT scheme, the matrix element of the electromagnetic current J_μ is reduced as [34]

$$\langle \mathcal{T}(p') | J_\mu | \mathcal{T}(p) \rangle = \bar{u}^\rho(p') \mathcal{O}_{\rho\mu\sigma}(p', p) u^\sigma(p), \quad (7)$$

with

$$\mathcal{O}_{\rho\mu\sigma}(p', p) = -g_{\rho\sigma} \left[v_\mu (F_1 - \tau F_2) + \frac{[S_\mu, S_\alpha]}{M_T} q^\alpha (F_1 + F_2) \right] - \frac{q^\rho q^\sigma}{4M_T^2} \left[v_\mu (F_3 - \tau F_4) + \frac{[S_\mu, S_\alpha]}{M_T} q^\alpha (F_3 + F_4) \right], \quad (8)$$

where $S_\mu = \frac{i}{2}\gamma_5 \sigma_{\mu\nu} v^\nu$ is the covariant spin-operator.

The tree and loop Feynman diagrams contributing to the magnetic moments are shown in Figs. 1 and 2, respectively. According to the standard power counting [30, 52], the chiral order D_χ of a Feynman diagram is

$$D_\chi = 2L + 1 + \sum_d (d-2)N_d^\phi + \sum_d (d-1)N_d^{\phi B} \quad (9)$$

where L , N_d^ϕ and $N_d^{\phi B}$ are the numbers of loops, pure meson vertices and meson-baryon vertices, respectively. d is the chiral dimension. The chiral order of the magnetic moment μ_T is counted as $(D_\chi - 1)$.

III. CHIRAL LAGRANGIANS

A. The leading order chiral Lagrangians

We choose the nonlinear realization of the chiral symmetry,

$$U = u^2 = \exp(i\phi/F_0), \quad (10)$$

where ϕ is the matrix for octet Goldstones,

$$\phi = \begin{pmatrix} \pi^0 + \frac{1}{\sqrt{3}}\eta & \sqrt{2}\pi^+ & \sqrt{2}K^+ \\ \sqrt{2}\pi^- & -\pi^0 + \frac{1}{\sqrt{3}}\eta & \sqrt{2}K^0 \\ \sqrt{2}K^- & \sqrt{2}\bar{K}^0 & -\frac{2}{\sqrt{3}}\eta \end{pmatrix}, \quad (11)$$

F_0 is the decay constant of the pseudoscalar meson in chiral limit. We adopt $F_\pi = 92.4$ MeV, $F_K = 113$ MeV and $F_\eta = 116$ MeV in this work. Under the $SU(3)_L \times SU(3)_R$ chiral transformation, the U and u respond according to

$$U \rightarrow RUL^\dagger, \quad (12)$$

$$u \rightarrow RuK^\dagger = KuL^\dagger, \quad (13)$$

where R and L are $SU(3)_R$ and $SU(3)_L$ transformation matrices, respectively. $K = K(R, L, \phi)$ is a unitary transformation.

We use the notations $B_{\bar{3}}$, B_6 and B_6^* to denote the antitriplet, spin- $\frac{1}{2}$ sextet and spin- $\frac{3}{2}$ sextet, respectively. These baryon fields are realized as [41]:

$$B_{\bar{3}} = \begin{pmatrix} 0 & \Lambda_c^+ & \Xi_c^+ \\ -\Lambda_c^+ & 0 & \Xi_c^0 \\ -\Xi_c^+ & -\Xi_c^0 & 0 \end{pmatrix}, \quad B_6 = \begin{pmatrix} \Sigma_c^{++} & \frac{\Sigma_c^+}{\sqrt{2}} & \frac{\Xi_c'^+}{\sqrt{2}} \\ \frac{\Sigma_c^+}{\sqrt{2}} & \Sigma_c^0 & \frac{\Xi_c'^0}{\sqrt{2}} \\ \frac{\Xi_c'^+}{\sqrt{2}} & \frac{\Xi_c'^0}{\sqrt{2}} & \Omega_c^0 \end{pmatrix}, \quad B_6^{*\mu} = \begin{pmatrix} \Sigma_c^{*++} & \frac{\Sigma_c^{*+}}{\sqrt{2}} & \frac{\Xi_c^{*+}}{\sqrt{2}} \\ \frac{\Sigma_c^{*+}}{\sqrt{2}} & \Sigma_c^{*0} & \frac{\Xi_c^{*0}}{\sqrt{2}} \\ \frac{\Xi_c^{*+}}{\sqrt{2}} & \frac{\Xi_c^{*0}}{\sqrt{2}} & \Omega_c^{*0} \end{pmatrix}^\mu \quad (14)$$

The chiral transformation can be established:

$$B \rightarrow KBK^T \quad (15)$$

where B represents the $B_{\bar{3}}$, the B_6 or the B_6^* field.

We introduce the left-handed and the right-handed external fields as the electromagnetic fields:

$$r_\mu = l_\mu = -eQ_{m(c)}A_\mu, \quad (16)$$

where A_μ is the electromagnetic field and $Q_{m(c)}$ represents the meson (singly charmed baryon) charge matrix. In this work, $Q_m = \text{diag}(2/3, -1/3, -1/3)$ and $Q_c = \text{diag}(1, 0, 0)$.

We define some ‘‘building blocks’’ before constructing Lagrangians. The chiral connection and axial vector field are defined as [30, 52],

$$\Gamma_\mu = \frac{1}{2} [u^\dagger(\partial_\mu - ir_\mu)u + u(\partial_\mu - il_\mu)u^\dagger], \quad (17)$$

$$u_\mu = \frac{i}{2} [u^\dagger(\partial_\mu - ir_\mu)u - u(\partial_\mu - il_\mu)u^\dagger], \quad (18)$$

The chiral covariant QED field strength tensors $F_{\mu\nu}^\pm$ are defined as

$$F_{\mu\nu}^\pm = u^\dagger F_{\mu\nu}^R u \pm u F_{\mu\nu}^L u^\dagger, \quad (19)$$

$$F_{\mu\nu}^R = \partial_\mu r_\nu - \partial_\nu r_\mu - i[r_\mu, r_\nu], \quad (20)$$

$$F_{\mu\nu}^L = \partial_\mu l_\nu - \partial_\nu l_\mu - i[l_\mu, l_\nu]. \quad (21)$$

In order to introduce the chiral symmetry breaking effect, we define χ_\pm ,

$$\begin{aligned} \chi_\pm &= u^\dagger \chi u^\dagger \pm u \chi^\dagger u, \\ \chi &= 2B_0 \text{diag}(m_u, m_d, m_s) \end{aligned} \quad (22)$$

where B_0 is a parameter related to the quark condensate and $m_{u,d,s}$ is the current quark mass.

The leading order ($\mathcal{O}(p^2)$) pure-meson Lagrangian is

$$\mathcal{L}_{\phi\phi}^{(2)} = \frac{F_0^2}{4} \langle \nabla_\mu U (\nabla^\mu U)^\dagger \rangle, \quad (23)$$

where the superscript denotes the chiral order. The $\langle X \rangle$ means the trace of field X . The covariant derivative of Goldstone fields is define as

$$\nabla_\mu U = \partial_\mu U - ir_\mu U + iUl_\mu. \quad (24)$$

The leading order Lagrangians for singly heavy baryons read

$$\begin{aligned} \mathcal{L}_{B\phi}^{(1)} &= \frac{1}{2} \langle \bar{B}_3 (i\not{D} - M_3) B_3 \rangle + \langle \bar{B}_6 (i\not{D} - M_6) B_6 \rangle \\ &+ \langle \bar{B}_6^{*\mu} [-g_{\mu\nu} (i\not{D} - M_{6^*}) + i(\gamma_\mu D_\nu + \gamma_\nu D_\mu) - \gamma_\mu (i\not{D} + M_{6^*}) \gamma_\nu] B_6^{*\nu} \rangle \\ &+ g_1 \langle \bar{B}_6 \gamma_\mu \gamma_5 u^\mu B_6 \rangle + g_2 \langle \bar{B}_6 \gamma_\mu \gamma_5 u^\mu B_3 + \text{H.c.} \rangle + g_3 \langle \bar{B}_{6\mu}^* u^\mu B_6 + \text{H.c.} \rangle \\ &+ g_4 \langle \bar{B}_{6\mu}^* u^\mu B_3 + \text{H.c.} \rangle + g_5 \langle \bar{B}_6^{*\nu} \gamma_\mu \gamma_5 u^\mu B_{6\nu}^* \rangle + g_6 \langle \bar{B}_3 \gamma_\mu \gamma_5 u^\mu B_3 \rangle, \end{aligned} \quad (25)$$

where g_i is the axial charge. In this work, we ignore the mass splitting among the particles in the same multiplet. M_3 , M_6 and M_{6^*} are the average baryon masses for the antitriplet, spin- $\frac{1}{2}$ sextet and spin- $\frac{3}{2}$ sextet, respectively.

In the framework of HBChPT, the leading order nonrelativistic Lagrangians read

$$\begin{aligned} \mathcal{L}_{B\phi}^{(1)} &= \frac{1}{2} \langle \bar{B}_3 i v \cdot D B_3 \rangle + \langle \bar{B}_6 (i v \cdot D - \delta_2) B_6 \rangle - \langle \bar{B}_6^* (i v \cdot D - \delta_3) B_6^* \rangle \\ &+ 2g_1 \langle \bar{B}_6 S \cdot u B_6 \rangle + 2g_2 \langle \bar{B}_6 S \cdot u B_3 + \text{H.c.} \rangle + g_3 \langle \bar{B}_{6\mu}^* u^\mu B_6 + \text{H.c.} \rangle \\ &+ g_4 \langle \bar{B}_{6\mu}^* u^\mu B_3 + \text{H.c.} \rangle + 2g_5 \langle \bar{B}_6^* S \cdot u B_6^* \rangle + 2g_6 \langle \bar{B}_3 S \cdot u B_3 \rangle, \end{aligned} \quad (26)$$

where we ignore the terms suppressed by $\frac{1}{M_T}$. $\delta_{1,2,3}$ are the mass differences between different multiplets,

$$\delta_1 = M_{6^*} - M_6, \quad \delta_2 = M_6 - M_3, \quad \delta_3 = M_{6^*} - M_3. \quad (27)$$

B. The next-to-leading order chiral Lagrangians

The $\mathcal{O}(p^2)$ baryon-photon Lagrangians contributing to the magnetic moments read:

$$\begin{aligned} \mathcal{L}_{B\gamma}^{(2)} &= \frac{d_2}{8M_N} \langle \bar{B}_3 \sigma^{\mu\nu} \hat{F}_{\mu\nu}^+ B_3 \rangle + \frac{d_3}{8M_N} \langle \bar{B}_3 \sigma^{\mu\nu} B_3 \rangle \langle F_{\mu\nu}^+ \rangle + \frac{d_5}{8M_N} \langle \bar{B}_6 \sigma^{\mu\nu} \hat{F}_{\mu\nu}^+ B_6 \rangle + \frac{d_6}{8M_N} \langle \bar{B}_6 \sigma^{\mu\nu} B_6 \rangle \langle F_{\mu\nu}^+ \rangle \\ &+ \frac{f_2}{8M_N} \langle \bar{B}_3 \sigma^{\mu\nu} \hat{F}_{\mu\nu}^+ B_6 \rangle + \text{H.c.} + \frac{if_4}{8M_N} \langle \bar{B}_3 \hat{F}_{\mu\nu}^+ \gamma^\nu \gamma^5 B_6^{*\mu} \rangle + \text{H.c.} + \frac{if_6}{8M_N} \langle \bar{B}_6 \hat{F}_{\mu\nu}^+ \gamma^\nu \gamma^5 B_6^{*\mu} \rangle + \text{H.c.} \\ &+ \frac{if_7}{8M_N} \langle \bar{B}_6 \gamma^\nu \gamma^5 B_6^{*\mu} \rangle \langle F_{\mu\nu}^+ \rangle + \text{H.c.} + \frac{if_9}{4M_N} \langle \bar{B}_6^{*\mu} \hat{F}_{\mu\nu}^+ B_6^{*\nu} \rangle + \frac{if_{10}}{4M_N} \langle \bar{B}_6^{*\mu} B_6^{*\nu} \rangle \langle F_{\mu\nu}^+ \rangle, \end{aligned} \quad (28)$$

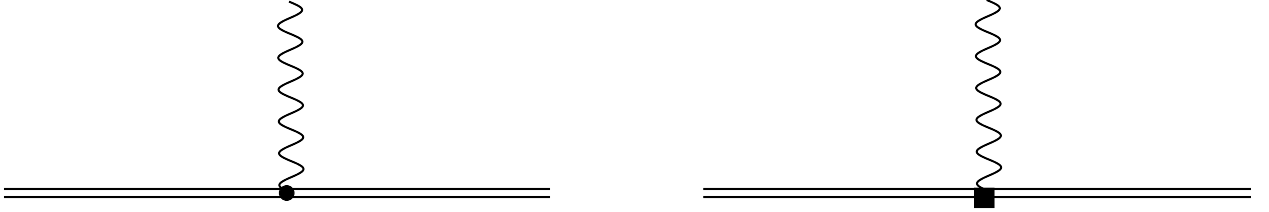


FIG. 1: The tree diagrams contribute to the magnetic moments of the spin- $\frac{3}{2}$ heavy baryon. The solid dot and black square represents $\mathcal{O}(p^2)$ and $\mathcal{O}(p^4)$ vertices, representatively.

where d_i and f_i are the coupling constants. $\hat{X} = X - \frac{1}{3}\langle X \rangle$ is the traceless part of the field X . The f_9 and f_{10} terms contribute to the leading order magnetic moments of spin- $\frac{3}{2}$ heavy baryons in the tree diagrams. Other terms will contribute to the higher order magnetic moments in the loop diagrams. The nonrelativistic form of Eq. (28) reads

$$\begin{aligned}
\mathcal{L}_{B\gamma}^{(2)} = & -\frac{id_2}{4M_N} \langle \bar{\mathcal{B}}_3[S^\mu, S^\nu] \hat{F}_{\mu\nu}^+ \mathcal{B}_3 \rangle - \frac{id_3}{4M_N} \langle \bar{\mathcal{B}}_3[S^\mu, S^\nu] \mathcal{B}_3 \rangle \langle F_{\mu\nu}^+ \rangle - \frac{id_5}{4M_N} \langle \bar{\mathcal{B}}_6[S^\mu, S^\nu] \hat{F}_{\mu\nu}^+ \mathcal{B}_6 \rangle \\
& - \frac{id_6}{4M_N} \langle \bar{\mathcal{B}}_6[S^\mu, S^\nu] \mathcal{B}_6 \rangle \langle F_{\mu\nu}^+ \rangle - \frac{if_2}{4M_N} \langle \bar{\mathcal{B}}_3[S^\mu, S^\nu] \hat{F}_{\mu\nu}^+ \mathcal{B}_6 \rangle + \text{H.c.} + \frac{if_4}{4M_N} \langle \bar{\mathcal{B}}_3 F_{\mu\nu}^+ S^\nu \mathcal{B}_6^{*\mu} \rangle + \text{H.c.} \\
& + \frac{if_6}{4M_N} \langle \bar{\mathcal{B}}_6 \hat{F}_{\mu\nu}^+ S^\nu \mathcal{B}_6^{*\mu} \rangle + \text{H.c.} + \frac{if_7}{4M_N} \langle \bar{\mathcal{B}}_6 S^\nu \mathcal{B}_6^{*\mu} \rangle \langle F_{\mu\nu}^+ \rangle + \text{H.c.} + \frac{if_9}{4M_N} \langle \bar{\mathcal{B}}_6^{*\mu} \hat{F}_{\mu\nu}^+ \mathcal{B}_6^{*\nu} \rangle \\
& + \frac{if_{10}}{4M_N} \langle \bar{\mathcal{B}}_6^{*\mu} \mathcal{B}_6^{*\nu} \rangle \langle F_{\mu\nu}^+ \rangle,
\end{aligned} \tag{29}$$

The d_2 terms in Eqs. (28) and (29) represent the contribution of the light degrees of freedom to the magnetic moments of the anti-triplet baryons. Since the J^P of the light diquark in the anti-triplet baryons is 0^+ , the M1 radiative transition $|J=0\rangle \rightarrow |J=0\rangle + \gamma$ is forbidden. The light diquark does not contribute to the magnetic moment and $d_2 = 0$.

We also construct the $\mathcal{O}(p^2)$ meson-meson-baryon interaction Lagrangian as followings, which contributes to the $\mathcal{O}(p^3)$ magnetic moments through the loop (j) in Fig 2.

$$\mathcal{L}_{B\phi\phi}^{(2)} = -\frac{f_8}{2M_N} \langle \bar{B}_6^{*\mu} [u_\mu, u_\nu] B_6^{*\nu} \rangle. \tag{30}$$

C. The higher order chiral Lagrangians

According to the group representation theory, there are seven interaction terms in $\mathcal{O}(p^4)$ Lagrangians which contribute to the $\mathcal{O}(p^3)$ magnetic moments in the tree diagrams [40]. The $\chi_+ = 4B_0 \text{diag}(0, 0, m_s) = 4B_0 m_s \tilde{\chi}_+$ at the leading order. We use the $\tilde{\chi}_+$ as the building block and the B_0 and m_s are absorbed into the LECs. There are only two independent nonvanishing terms

$$\mathcal{L}_{B\phi}^{(4)} = \frac{ih_2}{4M_N} \langle \bar{B}_6^{*\mu} \langle F_{\mu\nu}^+ \rangle \tilde{\chi}_+ B_6^{*\nu} \rangle + \frac{ih_4}{M_N} \langle \bar{B}_6^{*\mu} \hat{F}_{\mu\nu}^+ B_6^{*\nu} \tilde{\chi}_+^T \rangle. \tag{31}$$

IV. ANALYTICAL EXPRESSIONS

The leading order magnetic moments are at $\mathcal{O}(p)$, which stem from $\mathcal{O}(p^2)$ vertices in Eq. (29):

$$\mu_{\Sigma_c^{*++}}^{(1)} = -\left(\frac{2}{3}f_9 + f_{10}\right)\mu_N, \quad \mu_{\Sigma_c^{*+}}^{(1)} = \mu_{\Xi_c^{*+}}^{(1)} = -\left(\frac{1}{6}f_9 + f_{10}\right)\mu_N, \quad \mu_{\Sigma_c^{*0}}^{(1)} = \mu_{\Xi_c^{*0}}^{(1)} = \mu_{\Omega_c^{*0}}^{(1)} = \left(\frac{1}{3}f_9 - f_{10}\right)\mu_N. \tag{32}$$

There are two unknown LECs f_9 and f_{10} at this order.

Four loop diagrams (a)-(d) in Fig. 2 contribute to the $\mathcal{O}(p^2)$ magnetic moments. The meson-photon vertex arises from the $\mathcal{L}_{\phi\phi}^{(2)}$, while the meson-baryon vertex is from the $\mathcal{L}_{B\phi}^{(1)}$. The diagrams (c) and (d) vanish for the structure

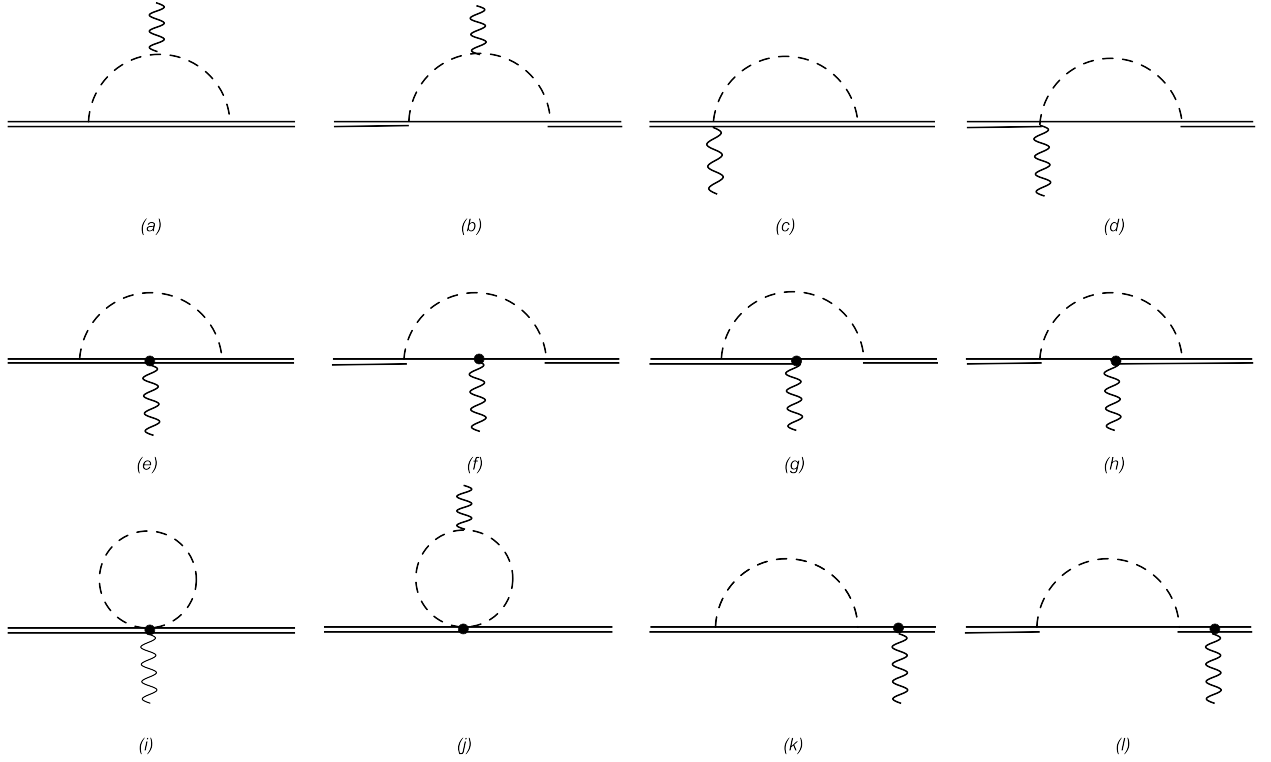


FIG. 2: The loop diagrams contribute to the magnetic moments of the spin- $\frac{3}{2}$ heavy baryons. The single and double lines represent the spin- $\frac{1}{2}$ and spin- $\frac{3}{2}$ heavy baryons, respectively. The solid dots denote the next-leading order vertices, while the other vertices are at the leading order. The diagrams (a)-(d) contribute to the $\mathcal{O}(p^2)$ magnetic moments, while the (e)-(l) diagrams contribute to the $\mathcal{O}(p^3)$ magnetic moments.

$v_\mu u^\mu$ in the amplitude [34, 37]. The corrections from the loops (a)-(d) read

$$\mu^{(2,a)} = \beta^\phi \frac{g_5^2 M_N}{2F_\phi^2} \frac{3-d}{d-1} n_1^{II}(0, m_\phi) \mu_N, \quad (33)$$

$$\mu^{(2,b)} = -\beta^\phi \frac{g_3^2 M_N}{4F_\phi^2} n_1^{II}(\delta_1, m_\phi) \mu_N - 2\beta^\phi \frac{g_4^2 M_N}{4F_\phi^2} n_1^{II}(\delta_3, m_\phi) \mu_N, \quad (34)$$

where the $n_1^{II}(\omega, m_\phi)$ is the loop integral given in Appendix A. The β^ϕ is the coefficient in Table I. There exist three LECs $g_{3,4,5}$ to be determined at this order.

The $\mathcal{O}(p^3)$ magnetic moments come from both the tree diagrams and the loop diagrams. The vertices of tree diagrams are from the interaction in Eq. (31). The results of the tree diagram read,

$$\begin{aligned} \mu_{\Sigma_c^{*++}}^{(3,\text{tree})} &= \mu_{\Sigma_c^{*+}}^{(3,\text{tree})} = \mu_{\Sigma_c^{*0}}^{(3,\text{tree})} = 0, \\ \mu_{\Xi_c^{*+}}^{(3,\text{tree})} &= -\left(\frac{1}{2}h_2 + \frac{4}{3}h_4\right) \mu_N, \quad \mu_{\Xi_c^{*0}}^{(3,\text{tree})} = -\left(\frac{1}{2}h_2 - \frac{2}{3}h_4\right) \mu_N, \quad \mu_{\Omega_c^{*0}}^{(3,\text{tree})} = -\left(h_2 - \frac{4}{3}h_4\right) \mu_N. \end{aligned} \quad (35)$$

The loop diagrams (e)-(l) in Fig. 2 contribute to the $\mathcal{O}(p^3)$ magnetic moments. The baryon-photon vertices in loop diagrams (e)-(h) come from the $\mathcal{L}_{B\gamma}^{(2)}$ in Eq. (29). The baryon-meson vertices are from the axial coupling Lagrangian in Eq. (26). The vertex in the loop diagram comes from the f_9 term in Eq. (29). The meson-meson-baryon vertex in the loop diagram (j) comes from the interaction (30). Diagrams (k) and (l) are the renormalization of the spin- $\frac{3}{2}$ baryon fields. The $\mathcal{O}(p^3)$ corrections from the above loop diagrams read,

$$\mu^{(3,i)} = 2\beta^\phi \frac{f_9 m_\phi^2}{128\pi^2 F_\phi^2} \ln \frac{m_\phi^2}{\lambda^2} \mu_N, \quad (36)$$

$$\mu^{(3,j)} = -4\beta^\phi \frac{f_8 m_\phi^2}{256\pi^2 F_\phi^2} \ln \frac{m_\phi^2}{\lambda^2} \mu_N, \quad (37)$$

TABLE I: The coefficients of the loop diagrams in Fig 2.

Loop		Σ_c^{*++}	Σ_c^{*+}	Σ_c^{*0}	Ξ_c^{*+}	Ξ_c^{*0}	Ω_c^{*0}	
(a),(b),	β^π	2		-2	1	-1		
(i),(j)	β^K	2	1			-1	-2	
(e)-(h)	γ_1^π	$\frac{5}{6}f_9 + 2f_{10}$	$\frac{1}{3}f_9 + 2f_{10}$	$-\frac{1}{6}f_9 + 2f_{10}$	$-\frac{1}{8}f_9 + \frac{3}{4}f_{10}$	$\frac{3}{4}f_{10}$		
	γ_1^K	$\frac{1}{6}f_9 + f_{10}$	$-\frac{1}{12}f_9 + f_{10}$	$-\frac{1}{3}f_9 + f_{10}$	$\frac{5}{12}f_9 + \frac{5}{2}f_{10}$	$-\frac{7}{12}f_9 + \frac{5}{2}f_{10}$	$-\frac{1}{6}f_9 + 2f_{10}$	
	γ_1^η	$\frac{2}{9}f_9 + \frac{1}{3}f_{10}$	$\frac{1}{18}f_9 + \frac{1}{3}f_{10}$	$-\frac{1}{9}f_9 + \frac{1}{3}f_{10}$	$\frac{1}{72}f_9 + \frac{1}{12}f_{10}$	$-\frac{1}{36}f_9 + \frac{1}{12}f_{10}$	$-\frac{4}{9}f_9 + \frac{4}{3}f_{10}$	
	γ_2^ϕ	$\gamma_2^\phi = \gamma_1^\phi (f_9 \rightarrow d_5, f_{10} \rightarrow d_6)$						
	γ_3^ϕ	$\gamma_3^\phi = \gamma_1^\phi (f_9 \rightarrow f_6, f_{10} \rightarrow f_7)$						
	ρ^π	$\frac{2}{3}d_2 + 4d_3$	$\frac{2}{3}d_2 + 4d_3$	$\frac{2}{3}d_2 + 4d_3$	$-\frac{1}{2}d_2 + 3d_3$	$3d_3$		
	ρ^K	$\frac{2}{3}d_2 + 4d_3$	$-\frac{1}{3}d_2 + 4d_3$	$-\frac{4}{3}d_2 + 4d_3$	$\frac{1}{3}d_2 + 2d_3$	$\frac{1}{3}d_2 + 2d_3$	$-\frac{2}{3}d_2 + 8d_3$	
	ρ^η				$\frac{1}{2}d_2 + 3d_3$	$-d_2 + 3d_3$		
	δ^π	-1		1	$\frac{1}{4}$	$\frac{1}{2}$		
	δ^K	-1	$-\frac{1}{2}$		$-\frac{1}{2}$	$\frac{1}{2}$	1	
	δ^η				$-\frac{1}{4}$			
	(k),(l)	ξ^π	2	2	2	$\frac{3}{4}$	$\frac{3}{4}$	
		ξ^K	1	1	1	$\frac{5}{2}$	$\frac{5}{2}$	2
ξ^η		$\frac{1}{3}$	$\frac{1}{3}$	$\frac{1}{3}$	$\frac{1}{12}$	$\frac{1}{12}$	$\frac{4}{3}$	
η^π		2	2	2	$\frac{3}{2}$	$\frac{3}{2}$		
η^K		2	2	2	1	1	4	
η^η					$\frac{3}{2}$	$\frac{3}{2}$		

$$\mu^{(3,e)} = \gamma_1^\phi \frac{g_5^2}{2F_\phi^2} \left(\frac{1-d}{2} + \frac{4}{d-1} - \frac{4}{(d-1)^2} \right) J_2'(0) \mu_N, \quad (38)$$

$$\mu^{(3,f)} = \gamma_2^\phi \frac{g_3^2}{4F_\phi^2} J_2'(\delta_1) \mu_N + \rho^\phi \frac{g_4^2}{4F_\phi^2} J_2'(\delta_3) \mu_N + 2\delta^\phi \frac{f_2 g_3 g_4}{4F_\phi^2} \frac{J_2(\delta_1) - J_2(\delta_3)}{\delta_1 - \delta_3} \mu_N, \quad (39)$$

$$\mu^{(3,g)} = \mu^{(3,h)} = \gamma_3^\phi \frac{g_5 g_3}{4F_\phi^2} \left(\frac{d-3}{d-1} \right) \frac{J_2(\delta_1) - J_2(0)}{(-\delta_1)} \mu_N + \delta^\phi \frac{g_5 g_4 f_4}{4F_\phi^2} \left(\frac{d-3}{d-1} \right) \frac{J_2(\delta_3) - J_2(0)}{(-\delta_3)} \mu_N, \quad (40)$$

$$\mu^{(3,k)} = \xi^\phi \frac{g_5^2}{F_\phi^2} J_2'(0) \left(\frac{1-d}{4} + \frac{1}{d-1} \right) \mu^{(1)}, \quad (41)$$

$$\mu^{(3,l)} = \xi^\phi \frac{-g_3^2}{4F_\phi^2} J_2'(\delta_1) \mu^{(1)} + \eta^\phi \frac{-g_4^2}{4F_\phi^2} J_2'(\delta_3) \mu^{(1)}, \quad (42)$$

where β^ϕ , γ_i^ϕ , ρ^ϕ , δ^ϕ , ξ^ϕ and η^ϕ are the coefficients of loops, which are given in Table I. There are thirteen new LECs introduced at this order.

V. INDEPENDENT LECS IN THE HEAVY QUARK LIMIT

There are eighteen unknown LECS in the analytical expressions in Eqs.(32)-(42), including five axial charges g_{1-5} , ten $\mathcal{O}(p^2)$ baryon-photon coupling constants $d_{2,3,5,6}$, $f_{2,4,6,7,9,10}$, one meson-meson-baryon coupling constant f_8 , and two $\mathcal{O}(p^4)$ chiral symmetry breaking coupling constants $h_{2,4}$. Since the number of the LECS is larger than that of the ground heavy baryons, we use the heavy quark symmetry to reduce the number of independent LECS.

The spin- $\frac{1}{2}$ and the spin- $\frac{3}{2}$ sextet are degenerate states in the heavy quark limit. The heavy quark symmetry can relate some LECS to others. We define a superfield \mathcal{H}_μ to denote \mathcal{B}_6 and $\mathcal{B}_{6\mu}^*$ [44, 47],

$$\mathcal{H}_\mu = \mathcal{B}_{6\mu}^* - \sqrt{\frac{1}{3}}(\gamma_\mu + v_\mu)\gamma^5\mathcal{B}_6, \quad (43)$$

$$\bar{\mathcal{H}}_\mu = \bar{\mathcal{B}}_{6\mu}^* + \sqrt{\frac{1}{3}}\bar{\mathcal{B}}_6\gamma^5(\gamma_\mu + v_\mu), \quad (44)$$

where $\bar{\mathcal{H}}_\mu$ is the conjugate field of \mathcal{H}_μ . v_μ is the velocity of heavy quark. In the heavy quark limit, the v_μ also corresponds to the velocity of the heavy baryon. This field \mathcal{H}_μ is constrained by

$$v \cdot \mathcal{H} = 0, \quad \not{v}\mathcal{H} = \mathcal{H}. \quad (45)$$

The \mathcal{H}_μ follows the same chiral transformation in Eq. (15).

In Refs. [44, 47], the authors constructed the axial coupling Lagrangian of the sextet baryons in heavy quark symmetry,

$$\mathcal{L}_{\mathcal{H}\phi}^{(1)} = ig_a\epsilon_{\mu\nu\rho\sigma}\langle\bar{\mathcal{H}}^\mu u^\rho v^\sigma \mathcal{H}^\nu\rangle + g_b\langle\bar{\mathcal{H}}^\mu u_\mu \mathcal{B}_3 + \text{H.c.}\rangle. \quad (46)$$

The LECS in $\mathcal{L}_{\mathcal{B}\phi}^{(1)}$ are reduced to two independent LECS, g_a and g_b :

$$g_5 = g_a, \quad g_1 = -\frac{2}{3}g_a, \quad g_3 = -\sqrt{\frac{1}{3}}g_a, \quad g_4 = g_b; \quad g_2 = -\sqrt{\frac{1}{3}}g_b, \quad g_6 = 0. \quad (47)$$

g_6 is the coupling constant between pseudoscalar mesons and antitriplet heavy baryons. The light spin $S_l = 0$ for the antitriplets. The pseudoscalar mesons only interact with the light degree in the heavy baryon. Thus, the parity and angular momentum conservation forbid the g_6 vertex.

The interaction in $\mathcal{L}_{\mathcal{B}\gamma}^{(2)}$ in heavy quark symmetry corresponds to

$$\mathcal{L}_{\mathcal{H}\gamma}^{(2)} = i\frac{g_c}{4M_N}\langle\bar{\mathcal{H}}^\mu \hat{F}_{\mu\nu}^+ \mathcal{H}^\nu\rangle - \frac{g_e}{4M_N}\epsilon^{\sigma\mu\nu\rho}\langle\bar{\mathcal{H}}_\sigma \hat{F}_{\mu\nu}^+ v_\rho \mathcal{B}_3\rangle + \text{H.c.} \quad (48)$$

The eight LECS $d_5, d_6, f_2, f_4, f_6, f_7, f_9$ and f_{10} in $\mathcal{L}_{\mathcal{B}\gamma}^{(2)}$ are reduced to two LECS g_c and g_e :

$$\begin{aligned} f_9 &= g_c, & f_6 &= \frac{2}{\sqrt{3}}g_c, & d_5 &= -\frac{2}{3}g_c, \\ f_{10} &= f_7 = d_6 = 0, \\ f_2 &= -\frac{2}{\sqrt{3}}g_e, & f_4 &= -4g_e. \end{aligned} \quad (49)$$

In Lagrangians, we decompose the $F_{\mu\nu}^+$ into the trace part $\langle F_{\mu\nu}^+ \rangle$ and traceless part $\hat{F}_{\mu\nu}^+$, which correspond to the contributions from the light quarks and the heavy quark, respectively. The contribution from the heavy quark to the magnetic moments is order of $\frac{1}{m_c}$. Thus, heavy quark contribution and the LECS, f_{10}, f_7 and d_6 vanish in the heavy quark limit.

For spin- $\frac{1}{2}$ singly heavy baryons, we construct the $\mathcal{O}(p^2)$ meson-baryon interaction and $\mathcal{O}(p^4)$ photon-baryon interaction [40]:

$$\mathcal{L}_{B\phi\phi}^{(2)} = \frac{id_4}{2M_N}\langle\bar{B}_6\sigma^{\mu\nu}[u_\mu, u_\nu]B_6\rangle, \quad (50)$$

$$\mathcal{L}_{B\gamma}^{(4)} = \frac{s_2}{8M_N}\langle\bar{B}_6\sigma^{\mu\nu}\langle F_{\mu\nu}^+\rangle\tilde{\chi}_+B_6\rangle + \frac{s_4}{2M_N}\langle\bar{B}_6\sigma^{\mu\nu}F_{\mu\nu}^+B_6\tilde{\chi}_+^T\rangle. \quad (51)$$

In the heavy quark symmetry, the LECS in Eqs. (50) and (51) can be related to those in Eqs. (30) and (31). The Lagrangians in the heavy quark limit read

$$\mathcal{L}_{\mathcal{H}\phi\phi}^{(2)} = \frac{g_f}{4M_N}\langle\bar{\mathcal{H}}^\mu[u_\mu, u_\nu]\mathcal{H}^\nu\rangle$$

TABLE II: The lattice QCD simulation results [20, 21, 23]. “√” represents the results used as input.

	Ξ_c^+	Ξ_c^0	Σ_c^{++}	Σ_c^0	$\Xi_c^{\prime+}$	$\Xi_c^{\prime0}$	Ω_c^0	Ω_c^{*0}
LQCD	0.235(25)	0.192(17)	1.499(202)	-0.875(103)	0.315(141)	-0.599(71)	-0.688(31)	-0.730(23)
SI Input	√	√	√		√		√	
SII Input	√	√	√		√		√	√
SIII Input	√	√	√		√		√	√

$$\mathcal{L}_{\mathcal{H}\gamma}^{(4)} = i \frac{g_h}{4M_N} \langle \bar{\mathcal{H}}^\mu \hat{F}_{\mu\nu}^+ \mathcal{H}^\nu \tilde{\chi}_+^T \rangle \quad (52)$$

The LECs are related as

$$d_4 = \frac{1}{6}g_f; \quad f_8 = -\frac{1}{2}g_f, \quad s_2 = h_2 = 0; \quad s_4 = -\frac{1}{6}g_h; \quad h_4 = \frac{g_h}{4}. \quad (53)$$

In the heavy quark limit, the heavy quark contribution vanishes. Thus, in this limit, there are seven nonvanishing independent LECs, d_2 and $g_{a,b,c,e,f,h}$, contributing to the magnetic moments of the sextet baryons.

VI. NUMERICAL RESULTS

In the present work, we perform the numerical analysis with three scenarios. In the first scenario, we use the LECs determined by our previous work [40]. Three new LECs, f_8 , h_2 and h_4 are related to d_4 , s_2 and s_4 through the heavy quark spin symmetry. In the second scenario, we reduce the number of the LECs in the heavy quark limit and adopt the lattice QCD simulation results as input. In the third scenario, we include the heavy quark contribution on the basis of the scenario II. As a by-product, we also give the magnetic moments of singly bottom baryon.

In the three scenarios, we all use the same axial coupling values. The axial coupling constants g_2 and g_4 in Eq. (26) are estimated through the decay widths of Σ_c and Σ_c^* , respectively [53, 54]. The other g_i are related to g_2 and g_4 with the help of quark model. Their values are

$$\begin{aligned} g_2 &= -0.60, & g_4 &= -\sqrt{3}g_2 = 1.04, & g_1 &= -\sqrt{\frac{8}{3}}g_2 = 0.98, \\ g_3 &= \frac{\sqrt{3}}{2}g_1 = 0.85, & g_5 &= -\frac{3}{2}g_1 = -1.47, & g_6 &= 0. \end{aligned} \quad (54)$$

A. Scenario I

In our previous work [40], we calculated the magnetic moments of the spin- $\frac{1}{2}$ singly heavy baryons. All the LECs in Eq. (29) have been evaluated through the quark model. Here, we review the idea in brief. The vertices in Eq. (29) contribute to the leading order (transition) magnetic moments in the HBChPT scheme. We assume that their values are approximate to those estimated by the naive quark model. Then, we can extract these LECs. The (transition) magnetic moments from the quark model and the leading order results in HBChPT are given in Table III and IV.

Apart from the axial coupling constants and the $\mathcal{O}(p^2)$ baryon-photon coupling constants, we have three new LECs in the present work. In our previous work, d_4 , s_2 and s_4 have been determined by fitting three lattice QCD results, $\mu_{\Sigma_c^{++}}$, $\mu_{\Xi_c^{\prime+}}$, and $\mu_{\Omega_c^0}$ in Table II. With the relations in Eq. (53), we obtain the values of f_8 , h_2 and h_4 . In this scenario, we keep the mass splitting between the spin- $\frac{1}{2}$ sextet and the spin- $\frac{3}{2}$ sextet. The mass splitting reads

$$\begin{aligned} \delta_1 &= M_{6^*} - M_6 = 67 \text{ MeV}, \\ \delta_2 &= M_6 - M_{\bar{3}} = 127 \text{ MeV}, \\ \delta_3 &= M_{6^*} - M_{\bar{3}} = 194 \text{ MeV}. \end{aligned} \quad (55)$$

We have determined all the LECs in the analytical expressions up to $\mathcal{O}(p^3)$. We give the numerical results in two schemes. In the first scheme, we include the spin- $\frac{1}{2}$ antitriplet, the spin- $\frac{1}{2}$, and the spin- $\frac{3}{2}$ sextet as the intermediate

TABLE III: The (transition) magnetic moments μ_{B_3} , $\mu_{B_6 \rightarrow B_3}$, and $\mu_{B_6^* \rightarrow B_3}$ from the quark model and the leading order results in HBChPT.

μ_{B_3}	Λ_c^+	Ξ_c^+	Ξ_c^0
QM	μ_c	μ_c	μ_c
$\mathcal{O}(p^1)$	$\frac{1}{3}d_2 + 2d_3$	$\frac{1}{3}d_2 + 2d_3$	$-\frac{2}{3}d_2 + 2d_3$
$\mu_{B_6 \rightarrow B_3}$	$\Sigma_c^+ \rightarrow \Lambda_c^+ \gamma$	$\Xi_c'^+ \rightarrow \Xi_c^+ \gamma$	$\Xi_c'^0 \rightarrow \Xi_c^0 \gamma$
QM	$\sqrt{\frac{1}{3}}(\mu_d - \mu_u)$	$\sqrt{\frac{1}{3}}(\mu_s - \mu_u)$	$\sqrt{\frac{1}{3}}(\mu_s - \mu_d)$
$\mathcal{O}(p^1)$	$\sqrt{\frac{1}{2}}f_2$	$\sqrt{\frac{1}{2}}f_2$	0
$\mu_{B_6^* \rightarrow B_3}$	$\Sigma_c^{*+} \rightarrow \Lambda_c^+ \gamma$	$\Xi_c^{*+} \rightarrow \Xi_c^+ \gamma$	$\Xi_c^{*0} \rightarrow \Xi_c^0 \gamma$
QM	$\frac{2}{\sqrt{6}}(\mu_u - \mu_d)$	$\frac{2}{\sqrt{6}}(\mu_u - \mu_s)$	$\frac{2}{\sqrt{6}}(\mu_d - \mu_s)$
$\mathcal{O}(p^1)$	$-\sqrt{\frac{1}{12}}f_4$	$-\sqrt{\frac{1}{12}}f_4$	0

TABLE IV: The (transition) magnetic moments μ_{B_6} , $\mu_{B_6^*}$ and $\mu_{B_6^* \rightarrow B_6}$ from the quark model and the leading order results in HBChPT.

μ_{B_6}	Σ_c^{++}	Σ_c^+	Σ_c^0	$\Xi_c'^+$	$\Xi_c'^0$	Ω_c^0
QM	$\frac{4}{3}\mu_u - \frac{1}{3}\mu_c$	$\frac{2}{3}\mu_u + \frac{2}{3}\mu_d - \frac{1}{3}\mu_c$	$\frac{4}{3}\mu_d - \frac{1}{3}\mu_c$	$\frac{2}{3}\mu_u + \frac{2}{3}\mu_s - \frac{1}{3}\mu_c$	$\frac{2}{3}\mu_d + \frac{2}{3}\mu_s - \frac{1}{3}\mu_c$	$\frac{4}{3}\mu_s - \frac{1}{3}\mu_c$
$\mathcal{O}(p^1)$	$\frac{2}{3}d_5 + d_6$	$\frac{1}{6}d_5 + d_6$	$-\frac{1}{3}d_5 + d_6$	$\frac{1}{6}d_5 + d_6$	$-\frac{1}{3}d_5 + d_6$	$-\frac{1}{3}d_5 + d_6$
$\mu_{B_6^*}$	Σ_c^{*++}	Σ_c^{*+}	Σ_c^{*0}	Ξ_c^{*+}	Ξ_c^{*0}	Ω_c^{*0}
QM	$2\mu_u + \mu_c$	$\mu_u + \mu_d + \mu_c$	$2\mu_d + \mu_c$	$\mu_u + \mu_s + \mu_c$	$\mu_d + \mu_s + \mu_c$	$2\mu_s + \mu_c$
$\mathcal{O}(p^1)$	$-\frac{2}{3}f_9 - f_{10}$	$-\frac{1}{6}f_9 - f_{10}$	$\frac{1}{3}f_9 - f_{10}$	$-\frac{1}{6}f_9 - f_{10}$	$\frac{1}{3}f_9 - f_{10}$	$\frac{1}{3}f_9 - f_{10}$
$\mu_{B_6^* \rightarrow B_6}$	$\Sigma_c^{*++} \rightarrow \Sigma_c^{++} \gamma$	$\Sigma_c^{*+} \rightarrow \Sigma_c^+ \gamma$	$\Sigma_c^{*0} \rightarrow \Sigma_c^0 \gamma$	$\Xi_c^{*+} \rightarrow \Xi_c^+ \gamma$	$\Xi_c^{*0} \rightarrow \Xi_c^0 \gamma$	$\Omega_c^{*0} \rightarrow \Omega_c^0 \gamma$
QM	$\frac{2\sqrt{2}}{3}(\mu_u - \mu_c)$	$\frac{\sqrt{2}}{3}(\mu_u + \mu_d - 2\mu_c)$	$\frac{2\sqrt{2}}{3}(\mu_d - \mu_c)$	$\frac{\sqrt{2}}{3}(\mu_u + \mu_s - 2\mu_c)$	$\frac{\sqrt{2}}{3}(\mu_d + \mu_s - 2\mu_c)$	$\frac{2\sqrt{2}}{3}(\mu_s - \mu_c)$
$\mathcal{O}(p^1)$	$-\sqrt{\frac{1}{6}}(\frac{2}{3}f_6 + f_7)$	$-\sqrt{\frac{1}{6}}(\frac{1}{6}f_6 + f_7)$	$-\sqrt{\frac{1}{6}}(-\frac{1}{3}f_6 + f_7)$	$-\sqrt{\frac{1}{6}}(\frac{1}{6}f_6 + f_7)$	$-\sqrt{\frac{1}{6}}(-\frac{1}{3}f_6 + f_7)$	$-\sqrt{\frac{1}{6}}(-\frac{1}{3}f_6 + f_7)$

states in the loops. The numerical results are listed in the left panel of Table V. The chiral convergence is not good enough. The $\mathcal{O}(p^3)$ contribution is larger than that at $\mathcal{O}(p^2)$ for Ξ_c^{*+} and Σ_c^{*0} . In the second scheme, we only take the spin- $\frac{1}{2}$ and spin- $\frac{3}{2}$ sextet as the intermediate states. The results are given in the right panel of Table V. The chiral convergence becomes much better.

The mass splittings $\delta_{1,2,3}$ do not vanish in the chiral limit, which will worsen the chiral convergence. Due to the large mass splitting δ_3 , about 194 MeV, including the spin- $\frac{1}{2}$ antitriplet will destroy the chiral convergence. As for the spin- $\frac{1}{2}$ sextet, the mass splitting δ_1 is small. Taking spin- $\frac{1}{2}$ sextet as intermediate states has almost no negative impact on the convergence. Meanwhile, the spin- $\frac{1}{2}$ and spin- $\frac{3}{2}$ sextet form doublet in the heavy quark limit. To calculate the magnetic moments of the spin- $\frac{3}{2}$ sextet, the contribution from the chiral fluctuation around the spin- $\frac{1}{2}$ sextet is important. Thus, we choose the results from the second scheme, in the right panel of Table V, as our final results.

B. Scenario II

According to Section V, we reduce the LECs to five unknown independent ones with the heavy quark symmetry. In this scenario, we make use of six lattice QCD results in Table II to determine them. In the heavy quark limit, the

TABLE V: The numerical results of spin- $\frac{3}{2}$ singly charmed baryon magnetic moments in the scenario I (in unit of μ_N). We take B_3 , B_6 and B_6^* as the intermediate states in the left panel, while we only consider the B_6 and B_6^* in the right panel.

SI	with B_3 , B_6 and B_6^*				with B_6 and B_6^*			
	$\mathcal{O}(p^1)$	$\mathcal{O}(p^2)$	$\mathcal{O}(p^3)$	Total	$\mathcal{O}(p^1)$	$\mathcal{O}(p^2)$	$\mathcal{O}(p^3)$	Total
Σ_c^{*++}	4.10	-1.16	-0.02	2.92	4.10	-1.03	-0.16	2.91
Σ_c^{*+}	1.48	-0.72	-0.17	0.59	1.48	-0.39	-0.10	0.99
Σ_c^{*0}	-1.13	-0.29	-0.32	-1.74	-1.13	0.26	-0.05	-0.92
Ξ_c^{*+}	1.48	0.14	-0.50	1.13	1.48	-0.13	-0.07	1.28
Ξ_c^{*0}	-1.13	0.58	-0.22	-0.77	-1.13	0.52	0.003	-0.61
Ω_c^{*0}	-1.13	1.45	-0.27	0.05	-1.13	0.78	0.08	-0.27

TABLE VI: The numerical results of spin- $\frac{3}{2}$ singly charmed baryon magnetic moments in the scenario II (in unit of μ_N). We take B_3 , B_6 and B_6^* as the intermediate states in the left panel, while we only consider the B_6 and B_6^* in the right panel.

SII	with B_3 , B_6 and B_6^*				with B_6 and B_6^*			
	$\mathcal{O}(p^1)$	$\mathcal{O}(p^2)$	$\mathcal{O}(p^3)$	Total	$\mathcal{O}(p^1)$	$\mathcal{O}(p^2)$	$\mathcal{O}(p^3)$	Total
Σ_c^{*++}	0.78	-1.28	2.43	1.92	2.63	-1.11	0.60	2.12
Σ_c^{*+}	0.19	-0.74	0.82	0.27	0.66	-0.39	0.18	0.44
Σ_c^{*0}	-0.39	-0.20	-0.78	-1.37	-1.32	0.32	-0.25	-1.24
Ξ_c^{*+}	0.19	0.10	-0.03	0.27	0.66	-0.16	0.03	0.52
Ξ_c^{*0}	-0.39	0.64	-1.28	-1.03	-1.32	0.55	-0.27	-1.03
Ω_c^{*0}	-0.39	1.49	-1.83	-0.73	-1.32	0.78	-0.26	-0.79

spin- $\frac{1}{2}$ and $\frac{3}{2}$ are degenerate states. The mass splittings are

$$\begin{aligned}\delta_1 &= M_{6^*} - M_6 = 0 \text{ MeV}, \\ \delta_2 &= \delta_3 = M_{6^{(*)}} - M_3 = 161 \text{ MeV}.\end{aligned}\tag{56}$$

In this scenario, we also apply two schemes to estimate the LECs. In the first scheme, we consider all the singly charmed baryons as the intermediate states. The results are given in the left panel of Table VI. In the second scheme, we set $g_e = 0$ and decouple the $\bar{3}_f$ and 6_f singly charmed baryon in the loop diagrams. The results are given in the right panel of Table VI.

The results in the left panel suffer from the bad convergence, which are even worse than those in the first scheme in the scenario I. The quark model predictions are comparable with the lattice QCD results. Taking the quark model results as the leading order input at least ensure a dominant $\mathcal{O}(p^1)$ contribution in scenario I. Comparing results in the two panels of Table VI, although the total values are similar, the chiral convergence in the second scheme improve significantly. Including the antitriplet as the intermediate states break the chiral convergence. Thus, we also choose the results from the second scheme as our final results in this scenario.

In the second scheme, the magnetic moments of sextet baryons do not depend on the antitriplet. In the sextet sector, we determine three unknown LECs and obtain twelve magnetic moments. Thus, this scenario has powerful predictions.

TABLE VII: The numerical results of spin- $\frac{3}{2}$ singly charmed baryon magnetic moments from the scenario III (in unit of μ_N). We take $B_{\bar{3}}$, B_6 and B_6^* as the intermediate states in the left panel, while we only take the B_6 and B_6^* in the right panel. The ‘‘HQ’’ represents the heavy quark contribution.

SIII	with $B_{\bar{3}}$, B_6 and B_6^*					with B_6 and B_6^*				
	HQ	$\mathcal{O}(p^1)$	$\mathcal{O}(p^2)$	$\mathcal{O}(p^3)$	Total	HQ	$\mathcal{O}(p^1)$	$\mathcal{O}(p^2)$	$\mathcal{O}(p^3)$	Total
Σ_c^{*++}	0.21	0.96	-1.28	2.65	2.54	0.21	2.69	-1.11	0.62	2.41
Σ_c^{*+}	0.21	0.24	-0.74	0.96	0.66	0.21	0.67	-0.39	0.18	0.67
Σ_c^{*0}	0.21	-0.48	-0.20	-0.73	-1.21	0.21	-1.35	0.32	-0.26	-1.07
Ξ_c^{*+}	0.21	0.24	0.10	0.27	0.81	0.21	0.67	-0.16	0.10	0.81
Ξ_c^{*0}	0.21	-0.48	0.64	-1.31	-0.94	0.21	-1.35	0.55	-0.31	-0.90
Ω_c^{*0}	0.21	-0.48	1.49	-1.94	-0.73	0.21	-1.35	0.78	-0.34	-0.70

C. Scenario III

In the lattice QCD simulation [20, 21, 23], the contribution of heavy quark and light quarks to the magnetic moments are given separately. The heavy quark contribution for Ξ_c^+ , Σ_c^{*+} , $\Xi_c'^+$, Ω_c^0 and Ω_c^{*0} read

$$\mu_{\Xi_c^+}^c = 0.226\mu_N, \quad \mu_{\Sigma_c^{*+}}^c = -0.066\mu_N, \quad \mu_{\Xi_c'^+}^c = -0.059\mu_N, \quad \mu_{\Omega_c^0}^c = -0.061\mu_N, \quad \mu_{\Omega_c^{*0}}^c = 0.239\mu_N, \quad (57)$$

where the superscript ‘‘c’’ denotes the contribution from the charm quark. According to the quark model in Tables III and IV, the heavy quark contribution is μ_c , $-\frac{1}{3}\mu_c$ and μ_c for the antitriplet, spin- $\frac{1}{2}$ sextet and spin- $\frac{3}{2}$ sextet, respectively. Using the lattice QCD results in Eqs. (57), we get the average $\mu_c = 0.205\mu_N$. In this scenario, the heavy quark contribution is estimated by using the average μ_c while the light quark contribution is derived through fitting the remaining part of lattice QCD results. The results are given in Table VII. The right panel of this table is our final results of this scenario.

The heavy quark contribution can also be introduced through the heavy quark symmetry breaking Lagrangian at $\mathcal{O}(1/m_c)$ which reads,

$$\mathcal{L}_{HQ} = \frac{g_H}{8M_N} \langle \bar{\mathcal{H}}^\rho \sigma_{\mu\nu} \mathcal{H}_\rho \rangle \langle F^{+\mu\nu} \rangle \quad (58)$$

The LECs d_6 , f_7 and f_{10} are related to g_H as

$$f_{10} = g_H, \quad d_6 = \frac{1}{3}g_H, \quad f_7 = -\frac{4}{\sqrt{3}}g_H. \quad (59)$$

We use the heavy quark contribution from the lattice QCD simulation to extract the g_H . The same magnetic moment results are obtained.

In scenario III, we can easily extend our formalism to calculate the magnetic moments of singly bottom baryons. In the heavy quark limit, the light contribution for a bottom baryon is the same as that for the charmed baryon. The heavy quark part is estimated using the quark model. We adopt the constituent mass $m_b = 4700$ MeV. The magnetic moments of singly bottom baryons are given in Table VIII.

VII. DISCUSSION AND CONCLUSION

We calculate the magnetic moments of spin- $\frac{3}{2}$ singly charmed baryons. The analytical expressions are derived up to $\mathcal{O}(p^3)$. There are eighteen unknown LECs involved. We reduce them into seven nonvanishing independent LECs with the heavy quark symmetry. Our numerical results are given up to $\mathcal{O}(p^3)$ in three scenarios. In the first scenario, we keep the mass difference between spin- $\frac{1}{2}$ and spin- $\frac{3}{2}$ sextet. The quark model results are regarded as the leading order magnetic moments. Five lattice QCD results are used to determine the LECs. The heavy quark symmetry is used to relate the $\mathcal{O}(p^2)$ $B\phi\phi$ and $\mathcal{O}(p^4)$ $B\gamma$ vertices to those for the spin- $\frac{1}{2}$ heavy baryons. In the second scenario, we adopt

TABLE VIII: The magnetic moments of singly bottom baryon sextet (in unit of μ_N). The “HQ” represents the heavy quark contribution. The light quark contribution is the same as that for singly charmed baryon.

spin- $\frac{1}{2}$			spin- $\frac{3}{2}$		
HQ	Total		HQ	Total	
Σ_b^+	0.02	1.59	Σ_b^{*+}	-0.06	2.14
Σ_b^0	0.02	0.39	Σ_b^{*0}	-0.06	0.40
Σ_b^-	0.02	-0.81	Σ_b^{*-}	-0.06	-1.35
Ξ_b^0	0.02	0.40	Ξ_b^{*0}	-0.06	0.54
Ξ_b^-	0.02	-0.73	Ξ_b^{*-}	-0.06	-1.17
Ω_b^-	0.02	-0.65	Ω_b^{*-}	-0.06	-0.97

TABLE IX: The numerical results of LECs for the three scenarios.

SI	d_2	d_3	f_9	f_6	d_5	f_{10}	f_7	d_6	d_4	f_8	s_2	h_2	s_4	h_4
	0.04	0.11	-5.23	-6.00	3.49	-0.61	0.60	0.03	3.45	-10.35	-0.24	0.36	-0.04	0.05
SII	d_2	d_3	g_c			f_{10}	f_7	d_6	g_f		s_2	h_2	g_h	
	-0.09	0	-3.95			0		0.61		0		0.32		
SIII	d_2	d_3	g_c			f_{10}	f_7	d_6	g_f		s_2	h_2	g_h	
	0.03	0.10	-4.04			-0.21	0.47	-0.07	0.41		0		0.12	

the heavy quark symmetry globally. The spin- $\frac{1}{2}$ and spin- $\frac{3}{2}$ sextets belong to the same doublet. The five unknown LECs are fitted using six lattice QCD results. In the third scenario, we add the heavy quark contribution explicitly on the basis of scenario II. In this scenario, we also evaluate the magnetic moments of singly bottom baryons as a by-product. Including the spin- $\frac{1}{2}$ antitriplet intermediate states will worsen the chiral divergence, due to its large mass difference with the sextet. We list both the results with all intermediate states and only sextet intermediate states. We take the latter ones as the final results.

We give our final results and those from other schemes in Table X. Compared with the scenario II, the scenario III includes the heavy quark contribution. The results in scenario III tend to be closer to those from other schemes. Thus, the $\frac{1}{m_c}$ effect may be not negligible. While the bottom quark is much heavier, its contribution in the singly

TABLE X: Comparison of the spin- $\frac{3}{2}$ singly charmed baryon magnetic in the literature, including the lattice QCD (LQCD) [21], the hyper central model (HCM) [11], effective mass (EM) and screened charge scheme (SC) [12], chiral constituent quark model (χ CQM) [10], light-cone QCD sum rules (LCQSR) [17], MIT bag model [13, 14], Skyrminion [15] scheme and chiral quark-soliton model (χ QSM) [19] (in unit of μ_N).

	SI	SII	SIII	LQCD	HCM	EM	SC	χ CQM	LCQSR	Bag I	Bag II	Skyrmion	χ QSM
Σ_c^{*++}	2.91	2.12	2.41	-	3.68 ~ 3.84	3.56	3.63	3.92	4.81 \pm 1.22	3.91	3.13	4.52 ~ 4.58	3.22 \pm 0.15
Σ_c^{*+}	0.99	0.44	0.67	-	1.20 ~ 1.26	1.17	1.18	0.97	2.00 \pm 0.46	1.34	1.09	1.12 ~ 1.31	0.68 \pm 0.04
Σ_c^{*0}	-0.92	-1.24	-1.07	-	-0.83 ~ -0.85	-1.23	-1.18	-1.99	-0.81 \pm 0.20	-1.20	-0.96	-2.29 ~ -1.92	-1.86 \pm 0.07
Ξ_c^{*+}	1.28	0.52	0.81	-	1.45 ~ 1.52	1.43	1.39	1.59	1.68 \pm 0.42	1.54	1.27	2.26 ~ 2.07	0.90 \pm 0.04
Ξ_c^{*0}	-0.61	-1.03	-0.90	-	-0.67 ~ -0.69	-1.00	-1.02	-1.43	-0.68 \pm 0.18	-1.01	-0.75	-2.01 ~ -1.98	-1.57 \pm 0.06
Ω_c^{*0}	-0.27	-0.79	-0.70	-0.73	-0.83 ~ -0.87	-0.77	-0.84	-0.86	-0.62 \pm 0.18	-0.78	-0.55	-0.87 ~ -1.23	-1.28 \pm 0.08

bottom baryons can be neglected. In the scenario I, no lattice QCD results for spin- $\frac{3}{2}$ heavy baryon is used as input. The value of $\mu_{\Omega_c^*0}$ in scenario I may become larger if we use lattice QCD simulation value as input. In the scenario III, we determined three unknown LECs and μ_c to give twelve predictions. The scenario III has powerful predictions with twelve predictions. Scenario I and III are quite different methods. The numerical results for the scenario I and III are similar and corroborate each other.

The other schemes in Table X include the lattice QCD [21], the hyper central model [11], effective mass and screened charge scheme [12], chiral constituent quark model [10], light-cone QCD sum rules [17], MIT bag model [13, 14], Skyrmion scheme [15] and chiral quark-soliton model [19]. Our results from all scenarios are less than those from other schemes in general. Same tendency also appeared in the magnetic moments of spin- $\frac{1}{2}$ charmed baryon [40]. In fact the lattice QCD results which we used as input are also less than other schemes. In the lattice QCD simulation, in order to extract the results with physical pion mass, the rough linear or quadratic extrapolation was used in Ref. [20].

We have calculated the magnetic moments of spin- $\frac{3}{2}$ singly heavy baryons analytically to $\mathcal{O}(p^3)$. The convergence of the chiral expansion is good in our numerical results. For the lack of experimental data, we have to adopt heavy quark symmetry and the quark model to reduce and estimate our LECs. Our numerical results can be improved with the new experimental results and the new lattice QCD simulation results in the future. Meanwhile, our analytical expressions can help the chiral extrapolation in lattice QCD simulation. The LECs determined in this work can also be used to study other physical properties, for instance, the electromagnetic decay of singly heavy baryon.

ACKNOWLEDGMENTS

L. Meng is very grateful to H. S. Li, X. L. Chen and W. Z. Deng for very helpful discussions. This project is supported by the National Natural Science Foundation of China under Grants 11575008, 11621131001 and 973 program. This work is also supported by the Fundamental Research Funds for the Central Universities of Lanzhou University under Grants 223000-862637.

Appendix A: Integrals

We give some integrals with the conditions $v \cdot q = 0$ and $q^2 = 0$. All the results are given in the dimension $d = 4$.

- Integrals with one meson propagator and one baryon propagator

$$i \int \frac{d^d l \lambda^{4-d}}{(2\pi)^d} \frac{l_\alpha l_\beta}{(l^2 - m^2 + i\epsilon)(\omega + v \cdot l + i\epsilon)} = g_{\alpha\beta} J_2(\omega) + v_\alpha v_\beta J_3(\omega) \quad (\text{A1})$$

$$J_2(\omega) = \begin{cases} \frac{2\omega(\omega^2 - m^2) + \omega(3m^2 - 2\omega^2) \left(\ln \frac{m^2}{\lambda^2} + 32\pi^2 L(\omega) \right) - 4(\omega^2 - m^2)^{3/2} (\cosh^{-1}(\frac{\omega}{m}) - i\pi)}{16\pi^2(d-1)} & (\omega > m) \\ \frac{2\omega(\omega^2 - m^2) + \omega(3m^2 - 2\omega^2) \left(\ln \frac{m^2}{\lambda^2} + 32\pi^2 L(\omega) \right) + 4(m^2 - \omega^2)^{3/2} \cos^{-1}(-\frac{\omega}{m})}{16\pi^2(d-1)} & (\omega^2 < m^2) \\ \frac{2\omega(\omega^2 - m^2) + \omega(3m^2 - 2\omega^2) \left(\ln \frac{m^2}{\lambda^2} + 32\pi^2 L(\omega) \right) + 4(\omega^2 - m^2)^{3/2} \cosh^{-1}(-\frac{\omega}{m})}{16\pi^2(d-1)} & (\omega < -m) \end{cases} \quad (\text{A2})$$

where $L(\lambda)$ is the infinite term:

$$L(\lambda) = \frac{\lambda^{d-4}}{16\pi^2} \left[\frac{1}{d-4} - \frac{1}{2} (\ln 4\pi + 1 + \Gamma'(1)) \right] \quad (\text{A3})$$

- Integrals with two meson propagators and one baryon propagator

$$i \int \frac{d^d l \lambda^{4-d}}{(2\pi)^d} \frac{l_\alpha l_\beta}{(l^2 - m^2 + i\epsilon)((l+q)^2 - m^2 + i\epsilon)(\omega + v \cdot l + i\epsilon)} = n_1^{\text{II}} g_{\alpha\beta} + n_2^{\text{II}} q_\alpha q_\beta + n_3^{\text{II}} v_\alpha v_\beta + n_4^{\text{II}} (v_\alpha q_\beta + q_\alpha v_\beta) \quad (\text{A4})$$

$$n_1^{\text{II}}(\omega) = \begin{cases} \frac{\omega(32\pi^2 L(\lambda) + \ln \frac{m^2}{\lambda^2}) + 2\sqrt{\omega^2 - m^2} (\cosh^{-1}(\frac{\omega}{m}) - i\pi)}{8\pi^2(d-2)} & (\omega > m) \\ \frac{\omega(32\pi^2 L(\lambda) + \ln \frac{m^2}{\lambda^2}) + 2\sqrt{m^2 - \omega^2} \cos^{-1}(-\frac{\omega}{m})}{8\pi^2(d-2)} & (\omega^2 < m^2) \\ \frac{\omega(32\pi^2 L(\lambda) + \ln \frac{m^2}{\lambda^2}) - 2\sqrt{\omega^2 - m^2} \cosh^{-1}(-\frac{\omega}{m})}{8\pi^2(d-2)} & (\omega < -m) \end{cases} \quad (\text{A5})$$

- Other integrals

The infinite terms are absorbed by the renormalization of the coefficients and the $L(\lambda)$ term is omitted in the following expression.

$$\frac{3-d}{d-1}n_1^{\text{II}}(\omega, m) = \begin{cases} -\frac{\omega(3\ln\frac{m^2}{\lambda^2}+1)+6\sqrt{\omega^2-m^2}[\cosh^{-1}(\frac{\omega}{m})-i\pi]}{144\pi^2} & (\omega > m) \\ -\frac{\omega(3\ln\frac{m^2}{\lambda^2}+1)+6\sqrt{m^2-\omega^2}\cos^{-1}(-\frac{\omega}{m})}{144\pi^2} & (\omega^2 < m^2) \\ -\frac{\omega(3\ln\frac{m^2}{\lambda^2}+1)-6\sqrt{\omega^2-m^2}\cosh^{-1}(-\frac{\omega}{m})}{144\pi^2} & (\omega < -m) \end{cases} \quad (\text{A6})$$

$$\frac{4}{d-1}n_1^{\text{II}}(\omega, m) = \begin{cases} \frac{\omega(3\ln\frac{m^2}{\lambda^2}-5)+6\sqrt{\omega^2-m^2}[\cosh^{-1}(\frac{\omega}{m})-i\pi]}{36\pi^2} & (\omega > m) \\ \frac{\omega(3\ln\frac{m^2}{\lambda^2}-5)+6\sqrt{m^2-\omega^2}\cos^{-1}(-\frac{\omega}{m})}{36\pi^2} & (\omega^2 < m^2) \\ \frac{\omega(3\ln\frac{m^2}{\lambda^2}-5)-6\sqrt{\omega^2-m^2}\cosh^{-1}(-\frac{\omega}{m})}{36\pi^2} & (\omega < -m) \end{cases} \quad (\text{A7})$$

$$J_2'(\omega) = \begin{cases} \frac{(m^2-2\omega^2)\ln(\frac{m^2}{\lambda^2})-4\omega\sqrt{\omega^2-m^2}[\cosh^{-1}(\frac{\omega}{m})-i\pi]+2\omega^2}{16\pi^2} & (\omega > m) \\ \frac{(m^2-2\omega^2)\ln(\frac{m^2}{\lambda^2})-4\omega\sqrt{m^2-\omega^2}\cos^{-1}(-\frac{\omega}{m})+2\omega^2}{16\pi^2} & (\omega^2 < m^2) \\ \frac{(m^2-2\omega^2)\ln(\frac{m^2}{\lambda^2})+4\omega\sqrt{\omega^2-m^2}\cosh^{-1}(-\frac{\omega}{m})+2\omega^2}{16\pi^2} & (\omega < -m) \end{cases} \quad (\text{A8})$$

$$\left(\frac{1-d}{4} + \frac{1}{d-1}\right)J_2'(\omega) = \begin{cases} \frac{-15(m^2-2\omega^2)\ln\frac{m^2}{\lambda^2}+60\omega\sqrt{\omega^2-m^2}[\cosh^{-1}(\frac{\omega}{m})-i\pi]-26m^2+22\omega^2}{576\pi^2} & (\omega > m) \\ \frac{-15(m^2-2\omega^2)\ln\frac{m^2}{\lambda^2}+60\omega\sqrt{m^2-\omega^2}\cos^{-1}(-\frac{\omega}{m})-26m^2+22\omega^2}{576\pi^2} & (\omega^2 < m^2) \\ \frac{-15(m^2-2\omega^2)\ln\frac{m^2}{\lambda^2}-60\omega\sqrt{\omega^2-m^2}\cosh^{-1}(-\frac{\omega}{m})-26m^2+22\omega^2}{576\pi^2} & (\omega < -m) \end{cases} \quad (\text{A9})$$

$$\left(\frac{1-d}{2} + \frac{4}{d-1} - \frac{4}{(d-1)^2}\right)J_2'(\omega) = \begin{cases} \frac{-33(m^2-2\omega^2)\ln\frac{m^2}{\lambda^2}+132\omega\sqrt{\omega^2-m^2}[\cosh^{-1}(\frac{\omega}{m})-i\pi]-70m^2+74\omega^2}{864\pi^2} & (\omega > m) \\ \frac{-33(m^2-2\omega^2)\ln\frac{m^2}{\lambda^2}+132\omega\sqrt{m^2-\omega^2}\cos^{-1}(-\frac{\omega}{m})-70m^2+74\omega^2}{864\pi^2} & (\omega^2 < m^2) \\ \frac{-33(m^2-2\omega^2)\ln\frac{m^2}{\lambda^2}-132\omega\sqrt{\omega^2-m^2}\cosh^{-1}(-\frac{\omega}{m})-70m^2+74\omega^2}{864\pi^2} & (\omega < -m) \end{cases} \quad (\text{A10})$$

Appendix B: Renormalization

In the HBChPT, the divergences from the loops with fixed order should be canceled out by renormalizing the LECs at this order. In this section, we calculate the divergences of the loop diagrams and give the renormalization of LECs explicitly. We take the mass splittings as

$$\delta_1 = 0, \quad \delta_2 = \delta_3 \equiv \delta. \quad (\text{B1})$$

We use the Gell-Mann-Okubo relation to express the η mass, $m_\eta^2 = (4m_K^2 - m_\pi^2)/3$. We adopt the leading order decay constants for mesons $F_\pi = F_K = F_\eta \equiv F_\phi$ for convenience.

The infinite parts of the $\mathcal{O}(p^3)$ loop diagrams (a) and (b) are

$$\mathbb{L}_6^{(3)} \sim -\frac{2}{3F_\phi^2}g_b^2M_N\delta\mathbb{A}_0L(\lambda); \quad \mathbb{L}_{6^*}^{(3)} \sim -\frac{1}{F_\phi^2}g_b^2M_N\delta\mathbb{A}_0L(\lambda). \quad (\text{B2})$$

where \mathbb{L} denotes the infinite terms. The subscripts 6 and 6* denote the spin- $\frac{1}{2}$ and spin- $\frac{3}{2}$ sextets, respectively. $\mathbb{A}_0 = \{4, 1, -2, 1, -2, -2\}$ corresponds to the loop coefficients of the sextet $\{\Sigma_c^{(*)++}, \Sigma_c^{(*)+}, \Sigma_c^{(*)0}, \Xi_c^{(*)+}, \Xi_c^{(*)0}, \Omega_c^{(*)0}\}$. The infinite parts in Eq. (B2) for two sextets can be cancelled simultaneously by one counter term,

$$\mathcal{L}_{\mathcal{H}\gamma}^{(3,ct)} = -i\frac{3g_b^2\delta L(\lambda)}{2F_\phi^2}\langle\bar{\mathcal{H}}^\mu\hat{F}_{\mu\nu}\mathcal{H}^\nu\rangle. \quad (\text{B3})$$

TABLE XI: The possible flavor structures of $\mathcal{O}(p^4)$ Lagrangian. $(\chi_+ f_{\mu\nu}^+)_{ab}^{ij} \equiv (\chi_+)_{\{a}^i (f_{\mu\nu}^+)_{b\}^j$, where the $\{\dots\}$ means that the flavor scripts are symmetrized.

Group representation	$1 \times 1 \rightarrow 1$	$1 \times 8 \rightarrow 8$	$8 \times 1 \rightarrow 8$	$8 \times 8 \rightarrow 1$	$8 \times 8 \rightarrow 8_1$	$8 \times 8 \rightarrow 8_2$	$8 \times 8 \rightarrow 27$
Flavor structure	$\langle \tilde{\chi}_+ \rangle \langle F_{\mu\nu}^+ \rangle$	$\langle \tilde{\chi}_+ \rangle \hat{F}_{\mu\nu}^+$	$\tilde{\chi}_+ \langle F_{\mu\nu}^+ \rangle$	$\langle \tilde{\chi}_+ \hat{F}_{\mu\nu}^+ \rangle$	$[\tilde{\chi}_+, \hat{F}_{\mu\nu}^+]$	$\{\tilde{\chi}_+, \hat{F}_{\mu\nu}^+\}$	$(\tilde{\chi}_+ \hat{F}_{\mu\nu}^+)_{\{a,b\}}^{\{i,j\}}$
LECs	$s_5/h_5/\kappa_5$	$s_6/h_6/\kappa_6$	$s_2/h_2/\kappa_2$	$s_3/h_3/\kappa_3$	-	$s_1/h_1/\kappa_1$	$s_4/h_4/\kappa_4$

TABLE XII: Coefficients of the magnetic moments that arise from the $\mathcal{O}(p^4)$ Lagrangians. The \mathbb{A}_i is also used to express the infinite parts of the $\mathcal{O}(p^4)$ loop diagrams.

	$\Sigma_c^{(*)++}$	$\Sigma_c^{(*)+}$	$\Sigma_c^{(*)0}$	$\Xi_c'^{(*)+}$	$\Xi_c'^{(*)0}$	$\Omega_c^{(*)0}$
\mathbb{A}_1	$\frac{4}{3N} m_\pi^2$	$\frac{1}{3N} m_\pi^2$	$-\frac{2}{3N} m_\pi^2$	$(-\frac{2}{3N} m_K^2 + \frac{1}{N} m_\pi^2)$	$-\frac{2}{3N} m_K^2$	$(-\frac{4}{3N} m_K^2 + \frac{2}{3N} m_\pi^2)$
\mathbb{A}_2	$\frac{m_\pi^2}{N}$	$\frac{m_\pi^2}{N}$	$\frac{m_\pi^2}{N}$	$\frac{m_K^2}{N}$	$\frac{m_K^2}{N}$	$\frac{2m_K^2 - m_\pi^2}{N}$
\mathbb{A}_3	$\frac{2}{3N} (m_K^2 - m_\pi^2)$	$\frac{2}{3N} (m_K^2 - m_\pi^2)$	$\frac{2}{3N} (m_K^2 - m_\pi^2)$	$\frac{2}{3N} (m_K^2 - m_\pi^2)$	$\frac{2}{3N} (m_K^2 - m_\pi^2)$	$\frac{2}{3N} (m_K^2 - m_\pi^2)$
\mathbb{A}_4	$\frac{8}{3N} m_\pi^2$	$\frac{2}{3N} m_\pi^2$	$-\frac{4}{3N} m_K^2$	$(\frac{8}{3N} m_K^2 - \frac{2}{N} m_\pi)$	$-\frac{4}{3N} m_K^2$	$(-\frac{8}{3} m_K^2 + \frac{4}{3N} m_\pi^2)$
\mathbb{A}_5	1	1	1	1	1	1
\mathbb{A}_6	$\frac{2}{3}$	$\frac{1}{6}$	$-\frac{1}{3}$	$\frac{1}{6}$	$-\frac{1}{3}$	$-\frac{1}{3}$

The divergences in the $\mathcal{O}(p^4)$ loop diagrams (e)-(l) should be absorbed by the LECs in the $\mathcal{O}(p^4)$ chiral Lagrangians. In Eq. (31), we set $m_u = m_d = 0$ and $\chi_+ = 4B_0 \text{diag}(0, 0, m_s) = 4B_0 m_s \tilde{\chi}_+$. In this section, we keep the u/d quark mass. At the lead order, the χ_+ reads:

$$\chi_+ = \text{diag}(m_\pi^2, m_\pi^2, 2m_K^2 - m_\pi^2), \quad \tilde{\chi}_+ = \frac{1}{N} \text{diag}(m_\pi^2, m_\pi^2, 2m_K^2 - m_\pi^2) \quad (\text{B4})$$

where $N = 2m_K^2 + m_\pi^2$. We have more nonvanishing independent terms in the $\mathcal{O}(p^4)$ Lagrangians than those in Eq. (31). As illustrated in Table XI, there are seven independent terms at this order. $[\tilde{\chi}_+, \hat{F}_{\mu\nu}^+]$ is vanishing at this order since the leading terms of $\tilde{\chi}_+$ and $\hat{F}_{\mu\nu}^+$ are both diagonal after the chiral expansion. We can reconstruct the $\mathcal{O}(p^4)$ Lagrangians for spin- $\frac{1}{2}$ and spin- $\frac{3}{2}$ sextets, respectively,

$$\begin{aligned} \mathcal{L}_{B\gamma}^{(4)} &= \frac{s_1}{8M_N} \langle \bar{B}_6 \sigma^{\mu\nu} \{\tilde{\chi}_+, \hat{F}_{\mu\nu}^+\} B_6 \rangle + \frac{s_2}{8M_N} \langle \bar{B}_6 \sigma^{\mu\nu} \tilde{\chi}_+ B_6 \rangle \langle F_{\mu\nu}^+ \rangle + \frac{s_3}{8M_N} \langle \bar{B}_6 \sigma^{\mu\nu} B_6 \rangle \langle \tilde{\chi}_+ \hat{F}_{\mu\nu}^+ \rangle \\ &+ \frac{s_4}{2M_N} \langle \bar{B}_6 \sigma^{\mu\nu} \hat{F}_{\mu\nu}^+ B_6 \tilde{\chi}_+^T \rangle + \frac{s_5}{8M_N} \langle \bar{B}_6 \sigma^{\mu\nu} B_6 \rangle \langle \tilde{\chi}_+ \rangle \langle F_{\mu\nu}^+ \rangle + \frac{s_6}{8M_N} \langle \bar{B}_6 \sigma^{\mu\nu} \langle \tilde{\chi}_+ \rangle \hat{F}_{\mu\nu}^+ B_6 \rangle, \end{aligned} \quad (\text{B5})$$

$$\begin{aligned} \mathcal{L}_{B^*\gamma}^{(4)} &= \frac{ih_1}{4M_N} \langle \bar{B}_6^{*\mu} \{\tilde{\chi}_+, \hat{F}_{\mu\nu}^+\} B_6^{*\nu} \rangle + \frac{ih_2}{4M_N} \langle \bar{B}_6^{*\mu} \tilde{\chi}_+ B_6^{*\nu} \rangle \langle F_{\mu\nu}^+ \rangle + \frac{ih_3}{4M_N} \langle \bar{B}_6^{*\mu} B_6^{*\nu} \rangle \langle \tilde{\chi}_+ \hat{F}_{\mu\nu}^+ \rangle \\ &+ \frac{ih_4}{M_N} \langle \bar{B}_6^{*\mu} \hat{F}_{\mu\nu}^+ B_6^{*\nu} \tilde{\chi}_+^T \rangle + \frac{ih_5}{4M_N} \langle \bar{B}_6^{*\mu} B_6^{*\nu} \rangle \langle \tilde{\chi}_+ \rangle \langle F_{\mu\nu}^+ \rangle + \frac{ih_6}{4M_N} \langle \bar{B}_6^{*\mu} \hat{F}_{\mu\nu}^+ B_6^{*\nu} \rangle \langle \tilde{\chi}_+ \rangle. \end{aligned} \quad (\text{B6})$$

The $h_2(s_2)$ and $h_5(s_5)$ terms involve the $\langle F_{\mu\nu}^+ \rangle$. The two terms represent the heavy quark's contribution. The other terms represent the light quarks' contribution. The magnetic moments of the spin- $\frac{1}{2}$ and spin- $\frac{3}{2}$ sextets are

$$\mu_6 = \sum_{i=1}^6 s_i \mathbb{A}_i, \quad \mu_{6^*} = - \sum_{i=1}^6 h_i \mathbb{A}_i, \quad (\text{B7})$$

where \mathbb{A}_i is the coefficients of h_i or s_i in Table XII. The divergences in the loop diagrams of spin- $\frac{1}{2}$ and spin- $\frac{3}{2}$ sextets can be absorbed by s_i and h_i , respectively.

The LECs h_i and s_i can be related to each other using the heavy quark expansion. In the heavy quark limit, the $\mathcal{O}(p^4)$ Lagrangians read

$$\begin{aligned}\mathcal{L}_{\mathcal{B}\gamma}^{(4)} &= \frac{i\kappa_1}{4M_N} \langle \bar{\mathcal{H}}^\mu \{ \tilde{\chi}_+, \hat{F}_{\mu\nu}^+ \} \mathcal{H}^\nu \rangle + \frac{i\kappa_3}{4M_N} \langle \bar{\mathcal{H}}^\mu \mathcal{H}^\nu \rangle \langle \tilde{\chi}_+ \hat{F}_{\mu\nu}^+ \rangle \\ &+ \frac{i\kappa_4}{M_N} \langle \bar{\mathcal{H}}^\mu \hat{F}_{\mu\nu}^+ \mathcal{H}^\nu \tilde{\chi}_+^T \rangle + \frac{i\kappa_6}{4M_N} \langle \bar{\mathcal{H}}^\mu \hat{F}_{\mu\nu}^+ \mathcal{H}^\nu \rangle \langle \tilde{\chi}_+ \rangle,\end{aligned}\quad (\text{B8})$$

where \mathcal{H}^μ is the superfield defined in Eq. (44). The heavy quark symmetry breaking Lagrangians at the order of $\frac{1}{m_c}$ read

$$\mathcal{L}_{HQ}^{(4)} = \frac{\kappa_2}{8M_N} \langle \bar{\mathcal{H}}^\rho \sigma_{\mu\nu} \tilde{\chi}_+ \mathcal{H}_\rho \rangle \langle F^{+\mu\nu} \rangle + \frac{\kappa_5}{8M_N} \langle \bar{\mathcal{H}}^\rho \sigma_{\mu\nu} \tilde{\chi}_+ \mathcal{H}_\rho \rangle \langle \tilde{\chi}_+ \rangle \langle F^{+\mu\nu} \rangle,\quad (\text{B9})$$

The $\mathcal{L}_{\mathcal{B}\gamma}^{(4)}$ and $\mathcal{L}_{HQ}^{(4)}$ describe the dynamics of the light quark and the heavy quark sectors, respectively. The s_i and h_i are related to the κ_i as

$$s_i = \begin{cases} -\frac{2}{3}\kappa_i & i = 1, 3, 4, 6 \\ \frac{1}{3}\kappa_i & i = 2, 5 \end{cases}, \quad h_i = \begin{cases} \kappa_i & i = 1, 3, 4, 6 \\ \kappa_i & i = 2, 5 \end{cases}, \Rightarrow s_i = \begin{cases} -\frac{2}{3}h_i & i = 1, 3, 4, 6 \\ \frac{1}{3}h_i & i = 2, 5 \end{cases}\quad (\text{B10})$$

Since the $\mathcal{O}(p^4)$ LECs of the spin- $\frac{1}{2}$ and spin- $\frac{3}{2}$ are related to each other as shown in Eq. (B10), we expect the divergences of the $\mathcal{O}(p^4)$ loop diagrams have the same relations.

Here we give the infinite parts of loop diagrams explicitly. For the spin- $\frac{1}{2}$ sextet, the divergences of the loops at $\mathcal{O}(p^4)$ are

$$\mathbb{L}_6^{(4)} \sim \sum_{i=1,3,4,6} a_i \mathbb{A}_i L(\lambda) + \sum_{i=2,5} a_i \mathbb{A}_i L(\lambda)\quad (\text{B11})$$

with

$$\begin{aligned}a_1 &= \frac{N}{12F_\phi^2} \left[g_c (8g_a^2 + 3g_b^2 + 6) - \frac{16}{3} g_a g_b g_e + 3g_f \right], \\ a_2 &= -\frac{N}{6F_\phi^2} g_b^2 (2d_3 + g_H), \\ a_3 &= \frac{N}{12F_\phi^2} [-8g_a g_b g_e + (3g_a^2 + 4)g_c + 2g_f], \\ a_4 &= \frac{N}{48F_\phi^2} \left(-\frac{40}{3} g_a g_b g_e + 7g_a^2 g_c + 6g_b^2 g_c \right), \\ a_5 &= \frac{8\delta^2 - N}{6F_\phi^2} g_b^2 (2d_3 + g_H), \\ a_6 &= \frac{N}{36F_\phi^2} [g_c (35g_a^2 + 36g_b^2 + 12) - 24g_a g_b g_e + 6g_f] + \frac{8}{3F_\phi^2} g_a g_b g_e \delta^2,\end{aligned}\quad (\text{B12})$$

where the a_2 and a_5 are related to the d_3 and g_H , which are coupling constants of the heavy quark sector. The other terms only involve the coupling constants of the light quark sector.

For the spin- $\frac{3}{2}$, the infinite parts of $\mathcal{O}(p^4)$ loop diagrams read

$$\mathbb{L}_{6^*}^{(4)} \sim \sum_{i=1,3,4,6} \frac{3}{2} a_i \mathbb{A}_i L(\lambda) - \sum_{i=2,5} 3a_i \mathbb{A}_i L(\lambda).\quad (\text{B13})$$

We find that

$$\mathbb{L}_{6,l}^{(4)} = \frac{2}{3} \mathbb{L}_{6^*,l}^{(4)}, \quad \mathbb{L}_{6,h}^{(4)} = -\frac{1}{3} \mathbb{L}_{6^*,h}^{(4)},\quad (\text{B14})$$

where the subscripts l and h represent the contributions from the light quarks and heavy quark, respectively. The divergences of the chiral loops respect the relations between s_i and h_i in the heavy quark limit (up to a -1 factor arising from Eq. (B7)). Even though the number of the LECs are reduced using the heavy quark symmetry, the divergences of the two sextets can be renormalized simultaneously. We give the renormalization of κ_i explicitly,

$$\kappa_i(\lambda) = \begin{cases} \kappa_i^{(r)} + \frac{3}{2} a_i L(\lambda) & i = 1, 3, 4, 6 \\ \kappa_i^{(r)} - 3a_i L(\lambda) & i = 2, 5 \end{cases}.\quad (\text{B15})$$

-
- [1] E. E. Jenkins and A. V. Manohar, Phys. Lett. **B335**, 452 (1994), hep-ph/9405431.
- [2] D. B. Leinweber, D.-H. Lu, and A. W. Thomas, Phys. Rev. **D60**, 034014 (1999), hep-lat/9810005.
- [3] E. J. Hackett-Jones, D. B. Leinweber, and A. W. Thomas, Phys. Lett. **B489**, 143 (2000), hep-lat/0004006.
- [4] L. S. Geng, J. Martin Camalich, L. Alvarez-Ruso, and M. J. Vicente Vacas, Phys. Rev. Lett. **101**, 222002 (2008), 0805.1419.
- [5] Y. Xiao, X.-L. Ren, J.-X. Lu, L.-S. Geng, and U.-G. Meiner, Eur. Phys. J. **C78**, 489 (2018), 1803.04251.
- [6] G.-J. Wang, R. Chen, L. Ma, X. Liu, and S.-L. Zhu, Phys. Rev. **D94**, 094018 (2016), 1605.01337.
- [7] Z.-G. Wang, Eur. Phys. J. **C78**, 297 (2018), 1712.05664.
- [8] D. B. Lichtenberg, Phys. Rev. **D15**, 345 (1977).
- [9] B. Julia-Diaz and D. O. Riska, Nucl. Phys. **A739**, 69 (2004), hep-ph/0401096.
- [10] N. Sharma, H. Dahiya, P. K. Chatley, and M. Gupta, Phys. Rev. **D81**, 073001 (2010), 1003.4338.
- [11] B. Patel, A. K. Rai, and P. C. Vinodkumar, J. Phys. **G35**, 065001 (2008), [J. Phys. Conf. Ser.110,122010(2008)], 0710.3828.
- [12] R. Dhir and R. C. Verma, Eur. Phys. J. **A42**, 243 (2009), 0904.2124.
- [13] S. K. Bose and L. P. Singh, Phys. Rev. **D22**, 773 (1980).
- [14] A. Bernotas and V. Simonis (2012), 1209.2900.
- [15] Y.-s. Oh, D.-P. Min, M. Rho, and N. N. Scoccola, Nucl. Phys. **A534**, 493 (1991).
- [16] S.-L. Zhu, W.-Y. P. Hwang, and Z.-S. Yang, Phys. Rev. **D56**, 7273 (1997), hep-ph/9708411.
- [17] T. M. Aliev, K. Azizi, and A. Ozpineci, Nucl. Phys. **B808**, 137 (2009), 0807.3481.
- [18] U. zdem (2018), 1804.10921.
- [19] G.-S. Yang and H.-C. Kim, Phys. Lett. **B781**, 601 (2018), 1802.05416.
- [20] K. U. Can, G. Erkol, B. Isildak, M. Oka, and T. T. Takahashi, JHEP **05**, 125 (2014), 1310.5915.
- [21] K. U. Can, G. Erkol, M. Oka, and T. T. Takahashi, Phys. Rev. **D92**, 114515 (2015), 1508.03048.
- [22] H. Bahtiyar, K. U. Can, G. Erkol, and M. Oka, Phys. Lett. **B747**, 281 (2015), 1503.07361.
- [23] H. Bahtiyar, K. U. Can, G. Erkol, M. Oka, and T. T. Takahashi, Phys. Lett. **B772**, 121 (2017), 1612.05722.
- [24] S. Weinberg, Physica **A96**, 327 (1979).
- [25] J. Gasser and H. Leutwyler, Annals Phys. **158**, 142 (1984).
- [26] J. Gasser and H. Leutwyler, Nucl. Phys. **B250**, 465 (1985).
- [27] E. E. Jenkins and A. V. Manohar, Phys. Lett. **B255**, 558 (1991).
- [28] V. Bernard, N. Kaiser, J. Kambor, and U. G. Meissner, Nucl. Phys. **B388**, 315 (1992).
- [29] E. E. Jenkins, M. E. Luke, A. V. Manohar, and M. J. Savage, Phys. Lett. **B302**, 482 (1993), [Erratum: Phys. Lett. B388,866(1996)], hep-ph/9212226.
- [30] V. Bernard, N. Kaiser, and U.-G. Meissner, Int. J. Mod. Phys. **E4**, 193 (1995), hep-ph/9501384.
- [31] U.-G. Meissner and S. Steininger, Nucl. Phys. **B499**, 349 (1997), hep-ph/9701260.
- [32] B. Kubis and U. G. Meissner, Eur. Phys. J. **C18**, 747 (2001), hep-ph/0010283.
- [33] S. J. Puglia and M. J. Ramsey-Musolf, Phys. Rev. **D62**, 034010 (2000), hep-ph/9911542.
- [34] H.-S. Li, Z.-W. Liu, X.-L. Chen, W.-Z. Deng, and S.-L. Zhu, Phys. Rev. **D95**, 076001 (2017), 1608.04617.
- [35] H.-S. Li, L. Meng, Z.-W. Liu, and S.-L. Zhu, Phys. Rev. **D96**, 076011 (2017), 1707.02765.
- [36] H.-S. Li, L. Meng, Z.-W. Liu, and S.-L. Zhu, Phys. Lett. **B777**, 169 (2018), 1708.03620.
- [37] L. Meng, H.-S. Li, Z.-W. Liu, and S.-L. Zhu, Eur. Phys. J. **C77**, 869 (2017), 1710.08283.
- [38] M. C. Banuls, I. Scimemi, J. Bernabeu, V. Gimenez, and A. Pich, Phys. Rev. **D61**, 074007 (2000), hep-ph/9905488.
- [39] V. S. Zamiralov, in *Proceedings, 10th Lomonosov Conference on Elementary Particle Physics: Moscow, Russia, August 23-29, 2001* (2003), pp. 159–164, URL http://www.ictp.trieste.it/cgi-bin/ICTPpreprints/swish.11/swish-web.cgi?keywords=IC2001158*.
- [40] G.-J. Wang, L. Meng, H.-S. Li, Z.-W. Liu, and S.-L. Zhu, Phys. Rev. **D98**, 054026 (2018), 1803.00229.
- [41] T.-M. Yan, H.-Y. Cheng, C.-Y. Cheung, G.-L. Lin, Y. C. Lin, and H.-L. Yu, Phys. Rev. **D46**, 1148 (1992), [Erratum: Phys. Rev. D55,5851(1997)].
- [42] H.-Y. Cheng, C.-Y. Cheung, G.-L. Lin, Y. C. Lin, T.-M. Yan, and H.-L. Yu, Phys. Rev. **D47**, 1030 (1993), hep-ph/9209262.
- [43] H.-Y. Cheng, C.-Y. Cheung, G.-L. Lin, Y. C. Lin, T.-M. Yan, and H.-L. Yu, Phys. Rev. **D49**, 2490 (1994), hep-ph/9308283.
- [44] H.-Y. Cheng, C.-Y. Cheung, G.-L. Lin, Y. C. Lin, T.-M. Yan, and H.-L. Yu, Phys. Rev. **D49**, 5857 (1994), [Erratum: Phys. Rev. D55,5851(1997)], hep-ph/9312304.
- [45] M. B. Wise, Phys. Rev. **D45**, R2188 (1992).
- [46] G. Burdman and J. F. Donoghue, Phys. Lett. **B280**, 287 (1992).
- [47] P. L. Cho and H. Georgi, Phys. Lett. **B296**, 408 (1992), [Erratum: Phys. Lett. B300,410(1993)], hep-ph/9209239.
- [48] T. Mehen and R. P. Springer, Phys. Rev. **D70**, 074014 (2004), hep-ph/0407181.
- [49] S. Nozawa and D. B. Leinweber, Phys. Rev. **D42**, 3567 (1990).
- [50] T. Ledwig, J. Martin-Camalich, V. Pascalutsa, and M. Vanderhaeghen, Phys. Rev. **D85**, 034013 (2012), 1108.2523.
- [51] W. Rarita and J. Schwinger, Phys. Rev. **60**, 61 (1941).
- [52] S. Scherer, Adv. Nucl. Phys. **27**, 277 (2003), [,277(2002)], hep-ph/0210398.
- [53] W. Meguro, Y.-R. Liu, and M. Oka, Phys. Lett. **B704**, 547 (2011), 1105.3693.
- [54] C. Patrignani et al. (Particle Data Group), Chin. Phys. **C40**, 100001 (2016).